PDR

EGG-SAAM-6381

August 1983

ANALYSIS OF THE APRIL 7, 1980 LOSS OF OFF-SITE POWER TRANSIENT AT ARKANSAS NUCLEAR ONE UNIT 1

C. B. Davis

Idaho National Engineering Laboratory
Operated by the U.S. Department of Energy

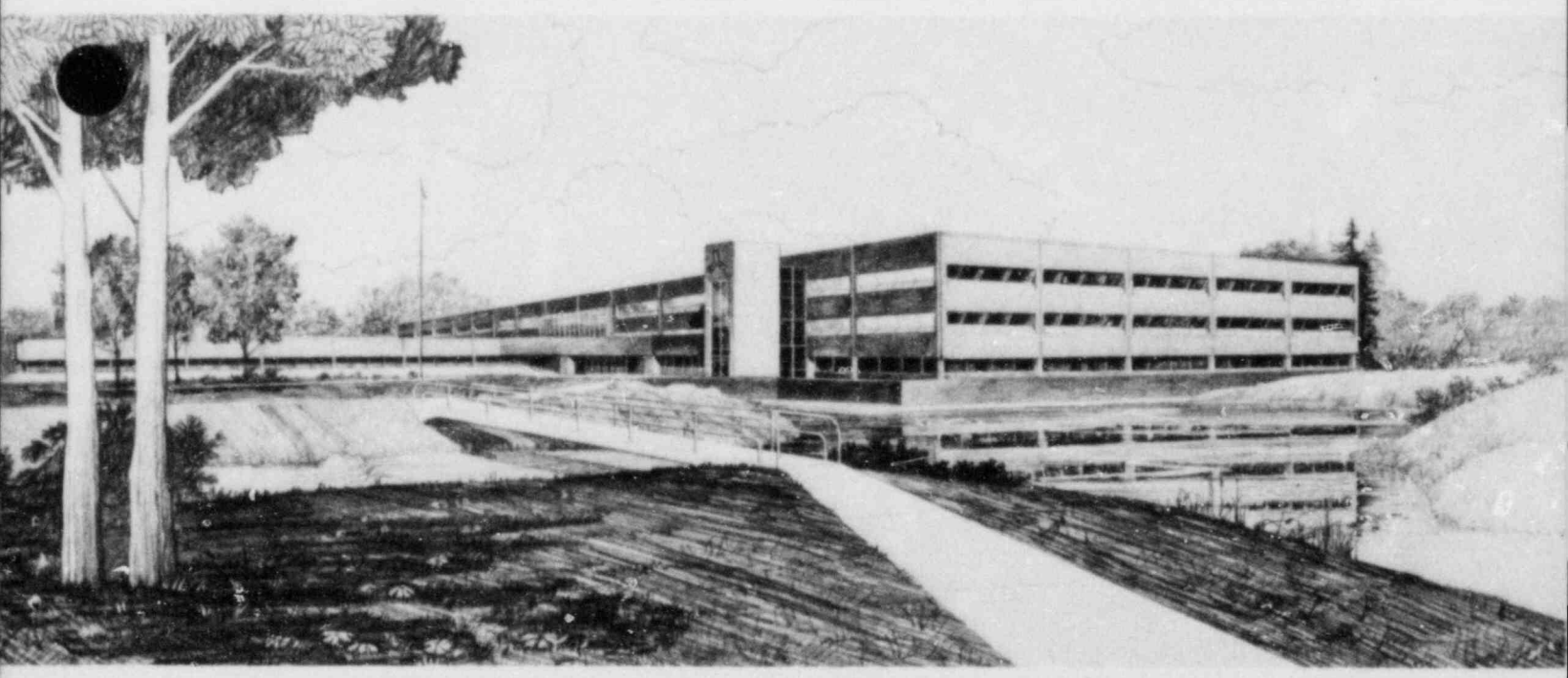

This is an informal report intended for use as a preliminary or working document

50-313

Prepared for the
U.S. NUCLEAR REGULATORY COMMISSION
Under DOE Contract No. DE-AC07-76ID01570
FIN No. A6270

EG&G Idaho

ABSTRACT

The loss of off-site power transient that occurred at Arkansas Nuclear One Unit 1 on April 7, 1980 was analyzed using the RELAP5 computer code. The transient was analyzed to understand the plant response, particularly in relation to natural circulation. Calculations were performed to determine the sensitivity of the plant response to high pressure injection, emergency feedwater, and the operation of the steam generator atmospheric dump valves. Methods of identifying the presence of natural circulation were investigated.

description. However, it was concluded that the reactor operators opened the atmospheric dump valves earlier than had been reported in the transient description.

The thermal-hydraulic response of the reactor coolant system was sensitive to the behavior of the steam generator and the operation of the high pressure injection system.

Natural circulation was fully established in the calculations when the coastdown of the reactor coolant pumps was completed. The magnitude of the calculated natural circulation flow was sensitive to the magnitude of the emergency feedwater flow. The natural circulation flow was modestly sensitive to high pressure injection and the operation of the atmospheric dump valves. The natural circulation flow was not sensitive to the cycling of the pressurizer electromatic relief valve. The calculations indicated that the presence of natural circulation could be inferred from temperature measurements, as discussed below. The cold leg temperature was closely coupled to the steam generator temperature during natural circulation. The hot leg temperature was also responsive to the steam generator temperature during natural circulation, although the response was delayed for a few minutes because of transit time effects. The difference between hot and cold leg temperatures stabilized shortly after natural circulation was established. Once natural circulation was established, the difference between hot and cold leg temperatures responded to changes in boundary conditions, such as starting or stopping emergency feedwater injection.

CONTENTS

FIGURES

TABLES

1. INTRODUCTION

The loss of off-site power (LOSP) transient that occurred at Arkansas Nuclear One Unit 1 (ANO-1) on April 7, 1980 was analyzed. The analysis was in support of case studies of natural circulation in commercial pressurized water reactors being performed by the Nuclear Regulatory Commission's Office for the Analysis and Evaluation of Operational Data. The principal analysis tool was the RELAP5 computer code. The objectives of the analysis were to understand the plant response during the LOSP, to identify and quantify possible operator actions that would explain the plant response, and to investigate natural circulation phenomena. The analysis was performed at the Idaho National Engineering Laboratory (INEL) by EG&G Idaho, Inc.

ANO-1 is a Babcock and Wilcox pressurized water reactor (PWR). ANO-1 is located near Russelville, Arkansas and is owned and operated by the Arkansas Power and Light Company. ANO-1 generates a gross electrical output of 880 MW and has a rated core thermal power of 2568 MW. The reactor coolant system contains two hot legs that connect the reactor vessel to two once-through steam generators. Each steam generator is connected to two cold legs that, in turn, are connected to the reactor vessel. Each cold leg contains a reactor coolant pump. The core contains 177 fuel assemblies in 15 x 15 fuel rod arrays and has an active height of 3.66 m (12 ft). Additional information on ANO-1 may be found in the Final Safety Analysis Report.[1]

A brief description of the LOSP transient, including major operator actions, is provided below. ANO-1 was operating at 100% core power on April 7, 1980 when tornado damage to offsite transmission towers resulted in a LOSP. The LOSP caused a reactor trip, turbine trip, and reactor coolant pump trip. After the LOSP, AC power was supplied by the diesel generators, one of which had been started prior to the LOSP. The turbine-driven and motor-driven emergency feedwater (EFW) pumps started automatically and delivered flow to the steam generators. The reactor operators manually initiated high pressure injection (HPI) to recover reactor coolant pressure and pressurizer level, which had decreased after

the reactor trip. Although one of the HPI isolation valves failed to open, cross connections between the injection lines allowed HPI flow into all four cold legs. Although manually throttled, HPI pressurized the reactor coolant to near the setpoint of the safety relief valves. The reactor operators then cycled the electromatic relief valve (ERV) on the pressurizer to prevent a challenge to the safety relief valves. The operators took manual control of emergency feedwater and used the atmospheric dump valves (ADVs) to vent steam from the steam generators. Off-site power was restored and the reactor coolant pumps were restarted about three hours after the LOSP. The unit was then returned to power operation. A more detailed scenario is presented in the transient description.[2]

The data presented in this report were digitized from strip charts recorded during the transient and presented in Reference 2. The uncertainties in the recorded data were not known. However, the uncertainty due to the digitization process can be estimated. Because of the large time scale on the strip charts, the uncertainty of the time scales due to the digitization is estimated to be 100 s. The uncertainty of the digitized maximum and minimum values of pressure, temperature, etc. is generally thought to be negligible. Consequently, emphasis should be placed on the trends of the data rather than the times at which events occurred or the slopes of the data.

RELAP5[3] is an advanced computer code designed for best estimate thermal-hydraulic analysis of postulated transients in light water reactors. RELAP5 is a one-dimensional analysis code based on a nonhomogeneous, nonequilibrium hydrodynamic model that utilizes one energy, two momentum, and two continuity equations. RELAP5 can represent horizontal stratified flow and subcooled or two-phase choked flow. In addition, RELAP5 has control systems to solve simultaneous algebraic and differential equations for simulating and controlling the behavior of components such as pumps and valves. The version of the code used in this analysis was RELAP5/MOD1.5 cycle 31, which has been stored under Configuration Control Number F01215 at the Computer Science Laboratory at the INEL.

The analysis of the LOSP transient at ANO-1 is one of several analyses being performed at the INEL to investigate natural circulation phenomena in PWRs. An analysis of a LOSP transient at Arkansas Nuclear One Unit 2, a Combustion Engineering PWR, was reported previously.[4] An analysis of a turbine trip experiment at Arkansas Nuclear One Unit 2 will be reported later. An analysis of a transient with loss of forced flow at McGuire 1, a Westinghouse PWR, will also be reported later.

A description of the RELAP5 model of ANO-1 is presented in Section 2 of this report. Results of the analysis of the LOSP transient are described in Section 3. Conclusions drawn from the analysis are presented in Section 4, and references are presented in Section 5.

2. MODEL DESCRIPTION

The RELAP5 model used in the analysis of the ANO-1 LOSP transient was modified from an existing model[5] of Oconee Unit 1. A comparison of the two units revealed that they were nearly identical except for the reactor coolant pumps and portions of the secondary coolant system. The Oconee model was modified to represent the Byron Jackson reactor coolant pumps used at ANO-1. The feed train and steam line portions of the secondary coolant system were also different between units. However, the differences between secondary coolant systems were not thought to be significant for a LOSP transient. Consequently the Oconee feed train and steam line models were not modified to represent the ANO-1 configuration. In addition to the reactor coolant pump model, various trips, initial conditions, and boundary conditions were altered to represent the ANO-1 LOSP transient.

The nodalization of the RELAP5 model of ANO-1 is described in Section 2.1 The initial conditions are described in Section 2.2, and the boundary conditions are described in Section 2.3.

2.1 Nodalization

The RELAP5 model of ANO-1 represented the major flow paths of the reactor coolant system and secondary coolant system. The emergency core coolant system, the pressurizer electromatic and safety relief valves, and pressurizer heaters and spray were modeled. The safety relief valves, atmospheric dump valves, turbine stop valves, and the main and emergency feedwater subsystems of the secondary coolant system were also modeled. The integrated control system (ICS) was modeled. The model contained 217 volumes, 231 junctions, and 204 heat structures and is shown schematically in Figures 1 through 9. Descriptions of the reactor coolant system, the secondary coolant system, and the ICS follow.

The nodalization of the coolant loops is shown in Figures 1 and 2. Each loop contained one hot leg, one steam generator, two reactor coolant pumps, and two cold legs. A high pressure injection (HPI) line was connected to each cold leg. The loops were designated as the A and B

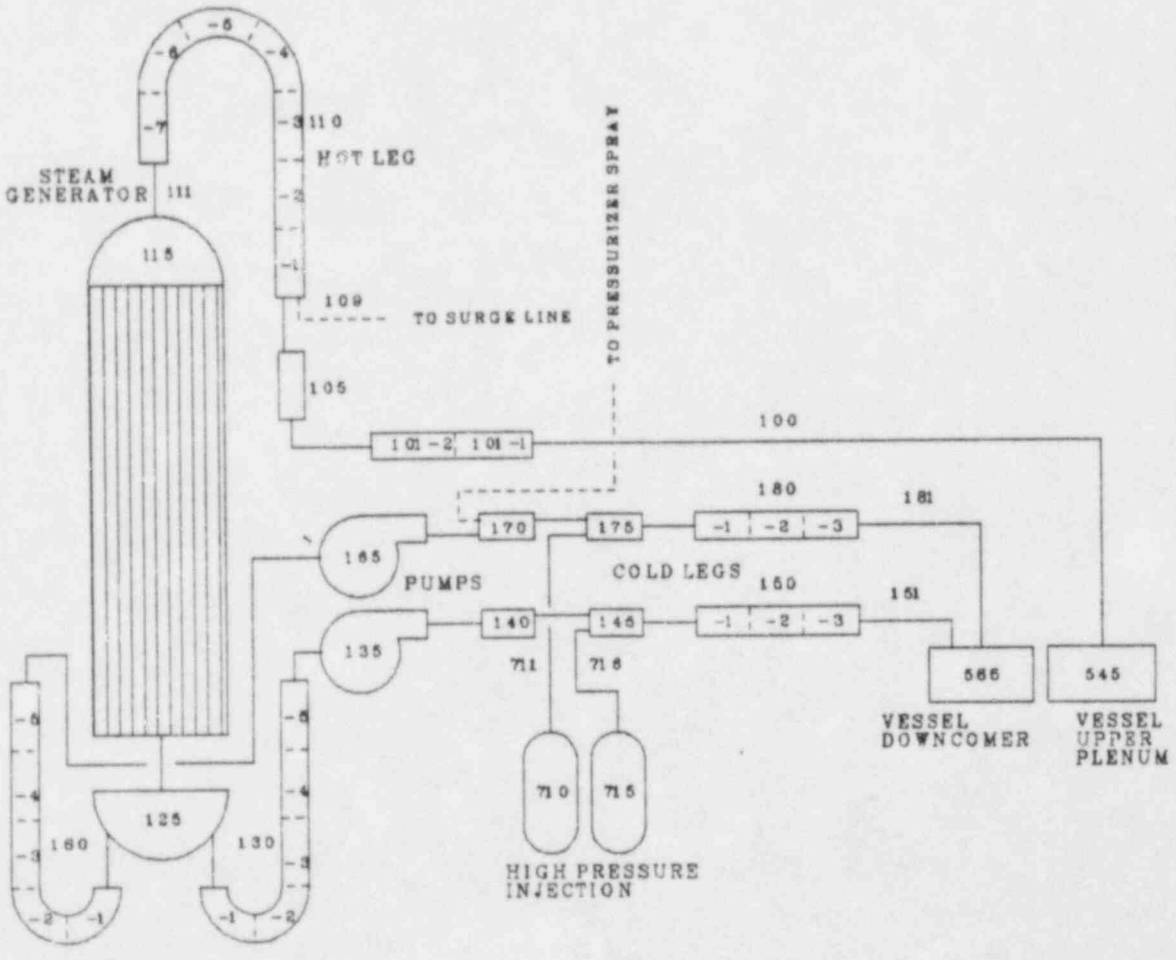

Figure 1. RELAP5 nodalization of the A coolant loop.

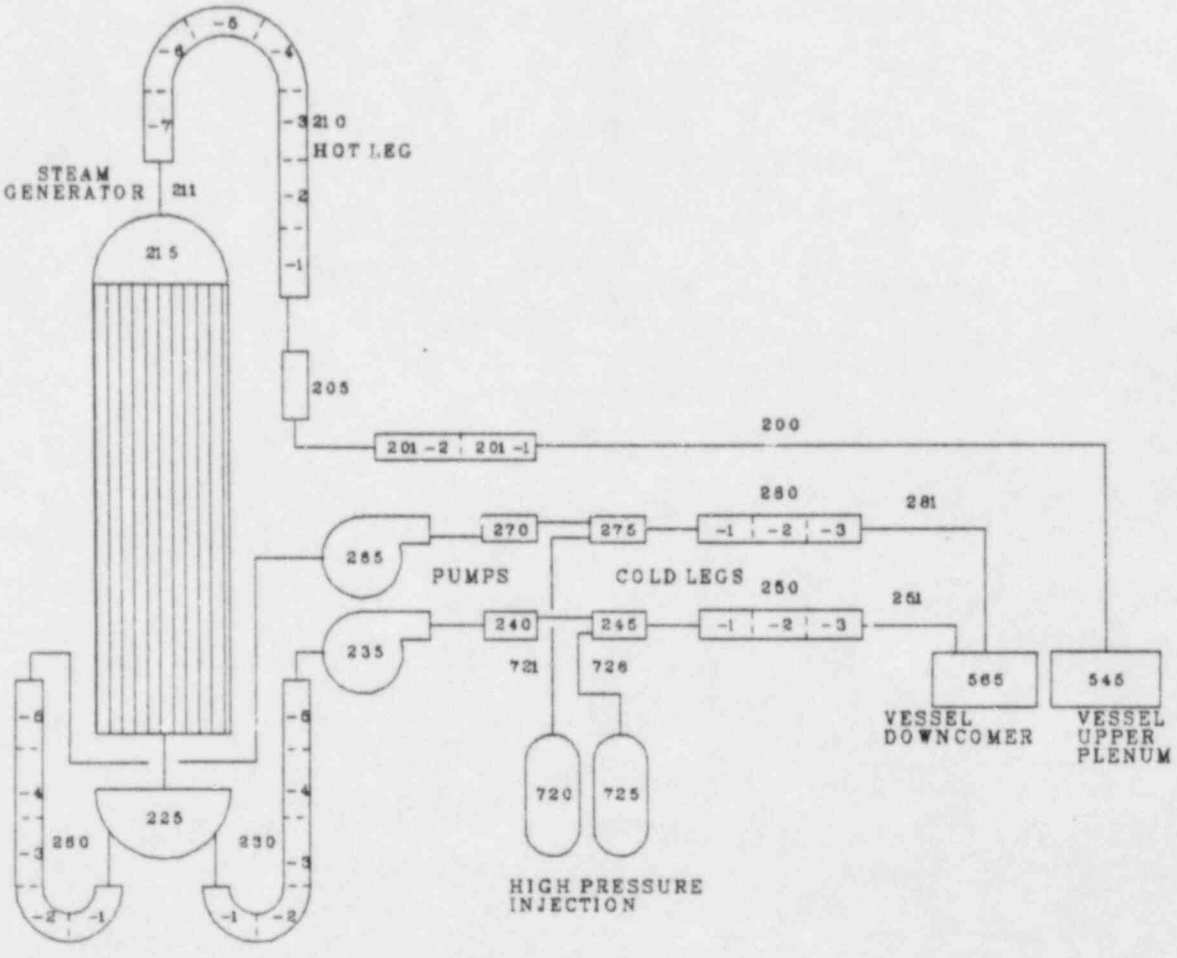

Figure 2. RELAP5 nodalization of the B coolant loop.

loops. The pressurizer was connected to the A loop. The pressurizer model, shown in Figure 3, contained representations of the surge line, electromatic relief valve (ERV), safety relief valves, heaters, and spray. The nodalization of the reactor vessel is shown in Figure 4. The vessel model contained representations of the downcomer, lower plenum, core, core bypass, upper plenum, upper head, and vent valves. The low pressure injection and core flood systems were connected to the downcomer. Heat structures were used to represent the stored energy in and the heat transfer from fuel rods, steam generator tubes, loop piping, vessel wall, vessel internals, pressurizer wall, surge line piping, and pressurizer heaters.

Nodalizations of the once-through steam generators are shown in Figures 5 and 6. The model contained representations of the steam generator tubes, downcomer, boiler, and steam outlet regions. Connections to the main feedwater, emergency feedwater, and the steam lines were represented. The turbine stop valves, the safety relief valves, and the atmospheric dump valves (ADVs) were also modeled. The eight safety relief valves on each steam line were represented as a single component in the RELAP5 model. A control system was used to compute the area of the RELAP5 valve as a function of the number of open relief valves, which was determined by the steam generator pressure. Heat structures were used to represent the stored energy in and heat transfer from the steam generator vessel wall and internals, including the steam generator tubes.

The nodalizations of the main feedwater and emergency feedwater systems are shown in Figures 7, 8, and 9. Heat structures were used to represent the high and low pressure feedwater heaters and the feedwater piping.

Portions of the ICS were represented. Specifically, the main feedwater, the emergency feedwater, and the turbine bypass/atmospheric dump valve control subsystems were represented.

A more detailed description of the RELAP5 model can be found in Reference 5.

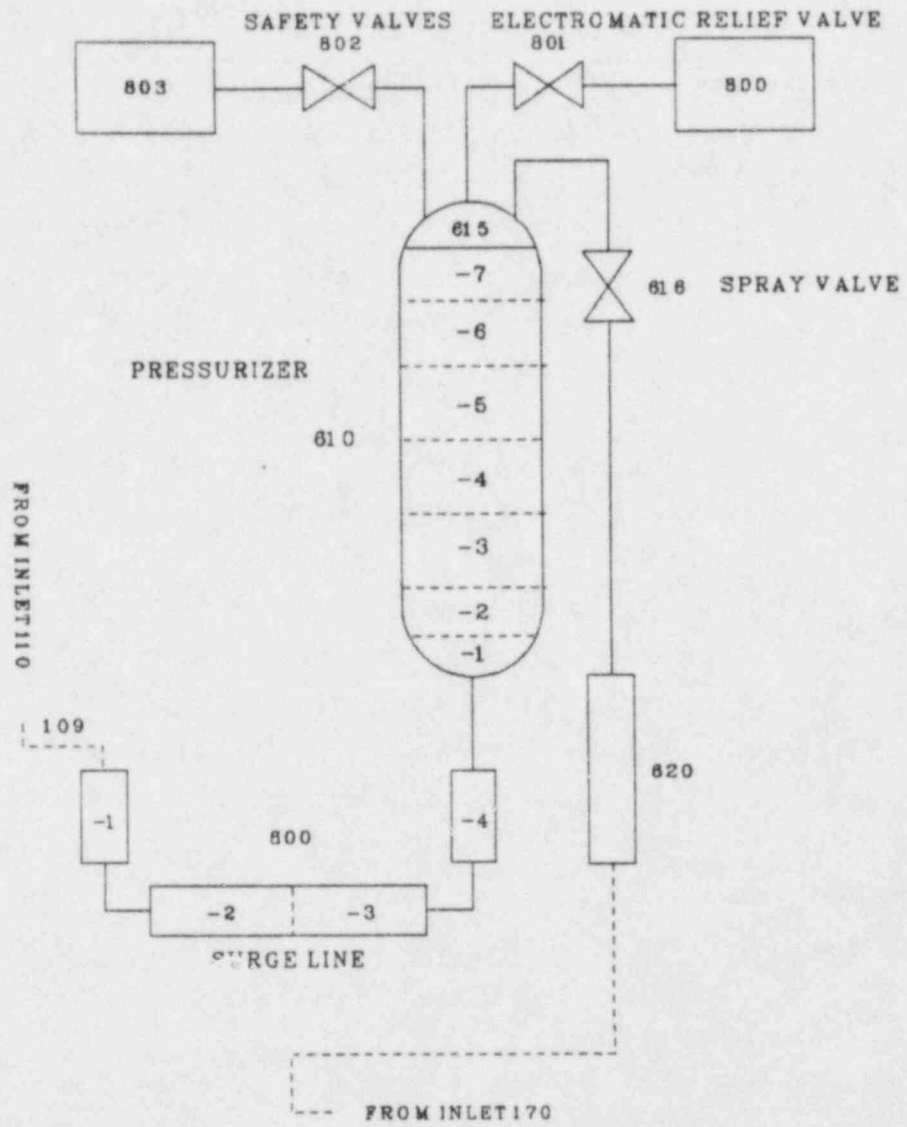

Figure 3. RELAP5 nodalization of the pressurizer.

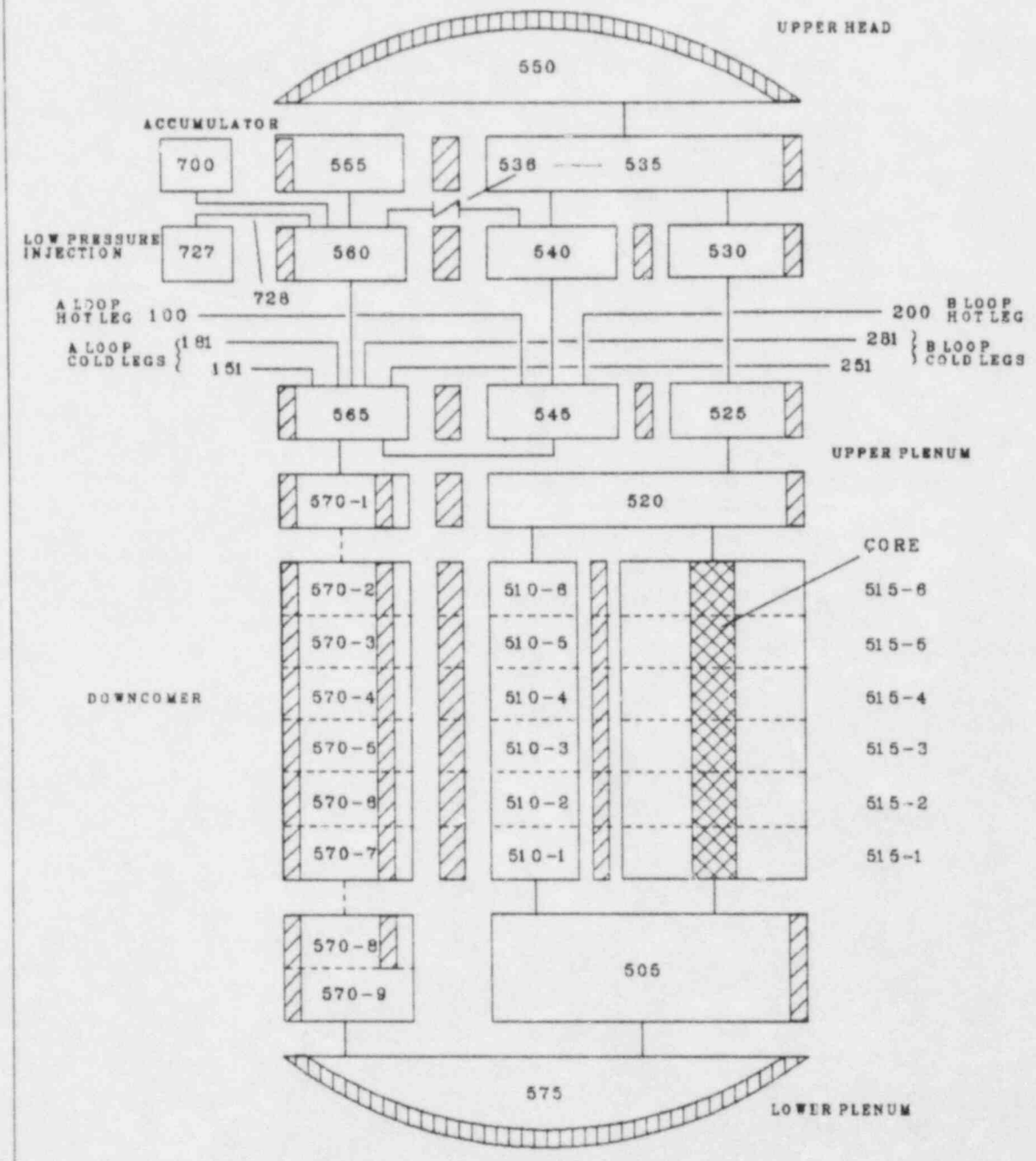

Figure 4. RELAP5 nodalization of the reactor vessel.

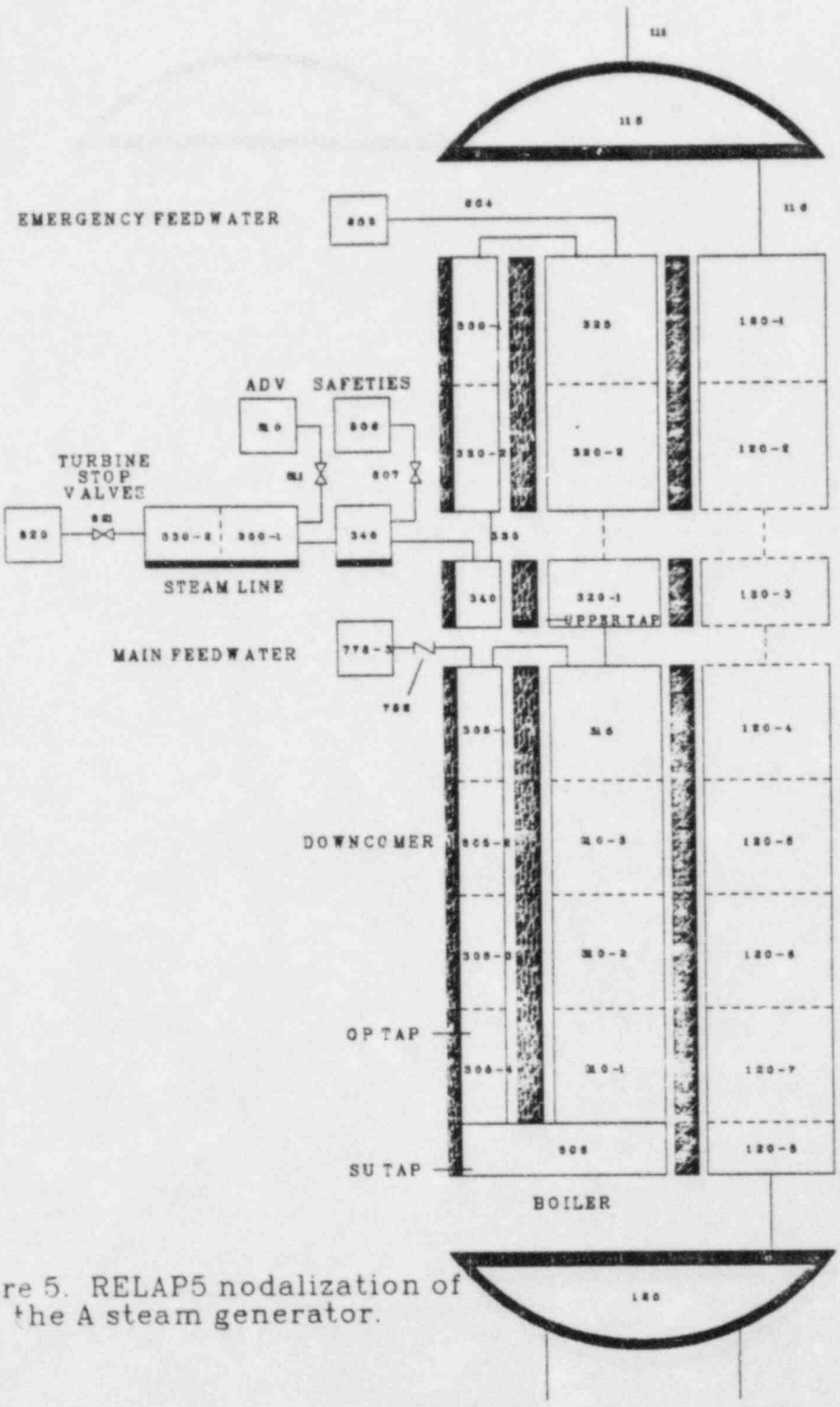

Figure 5. RELAP5 nodalization of the A steam generator.

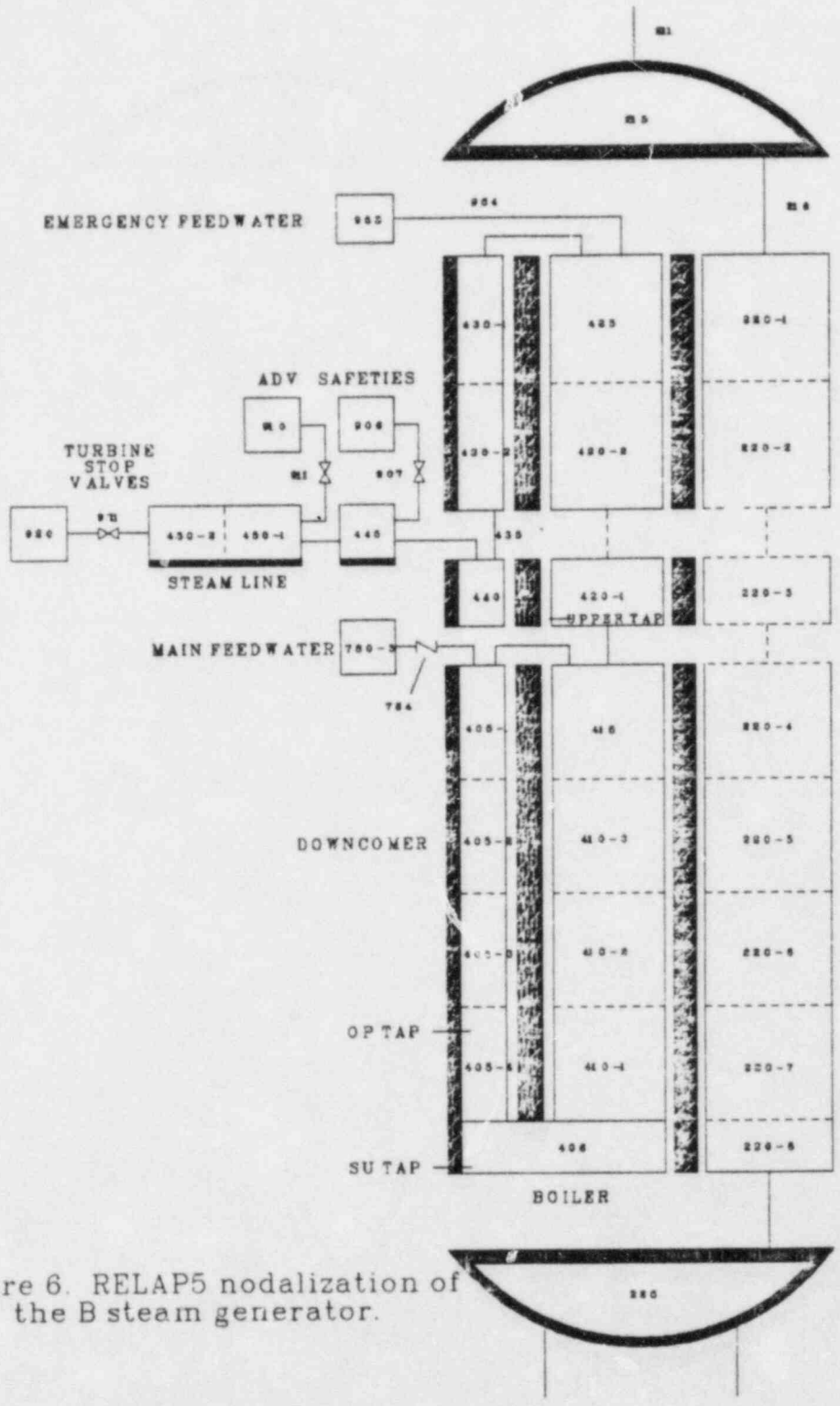

Figure 6. RELAP5 nodalization of the B steam generator.

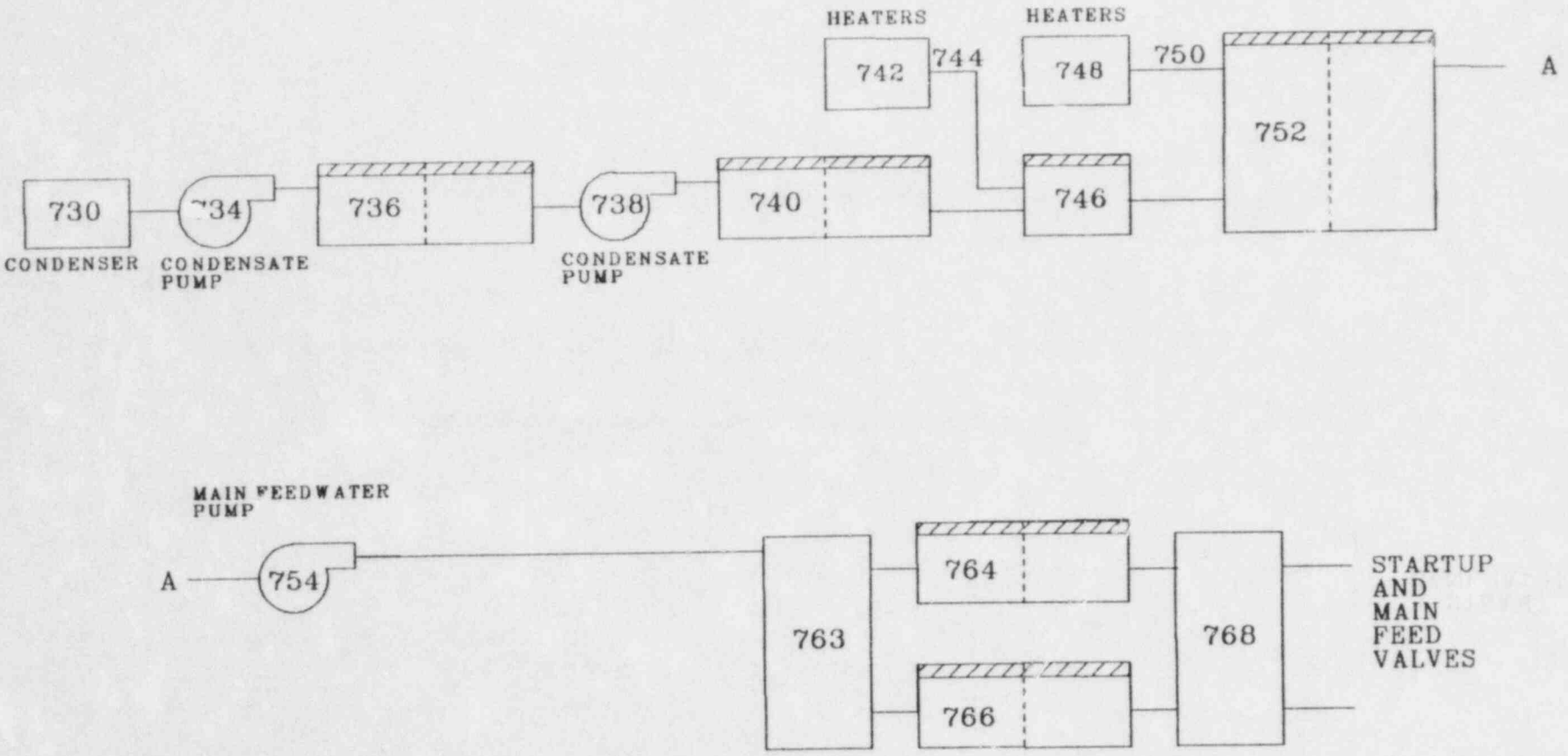

Figure 7. RELAP5 nodalization of the main feedwater system.

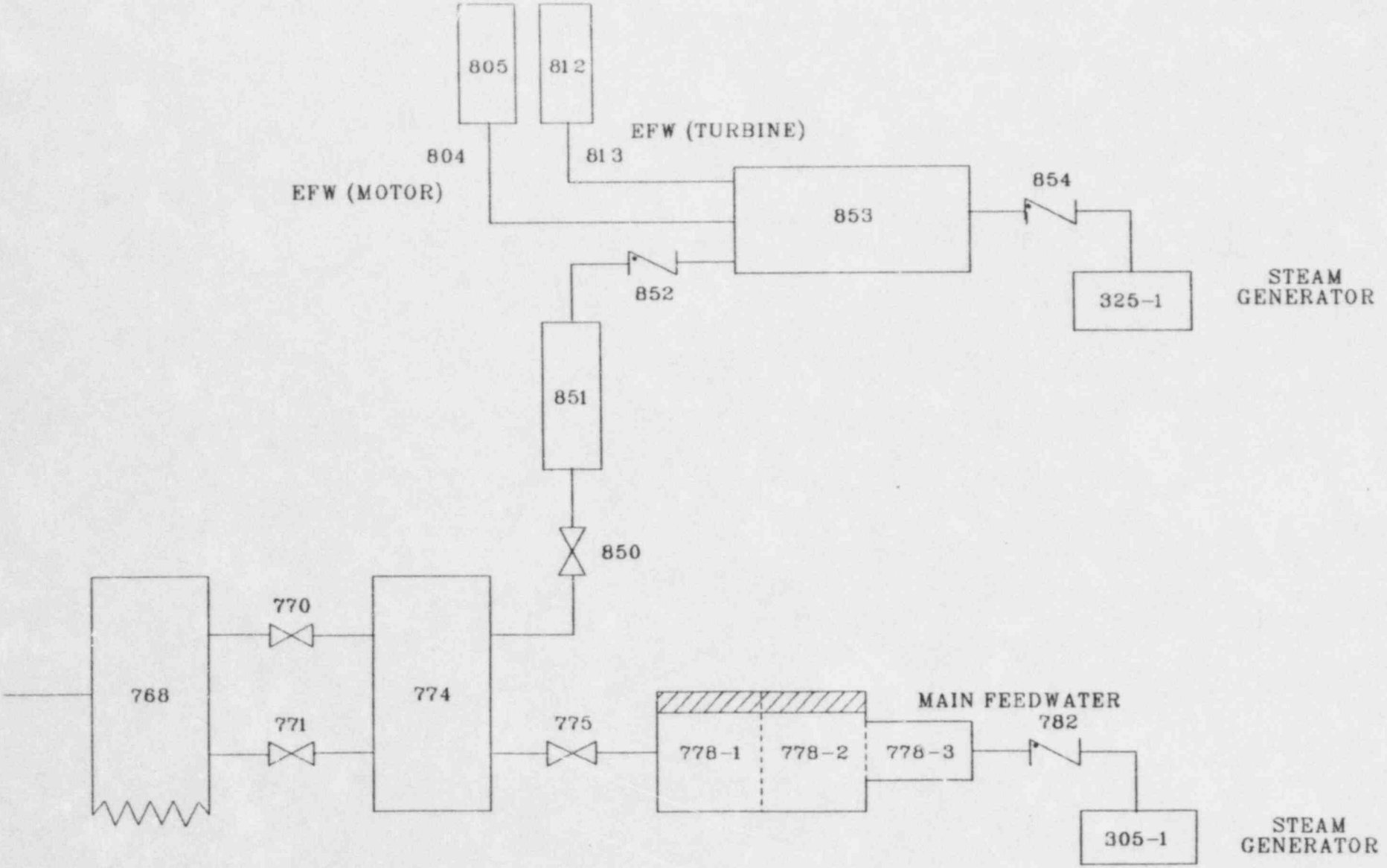

Figure 8. RELAP5 nodalization of the A feedwater header.

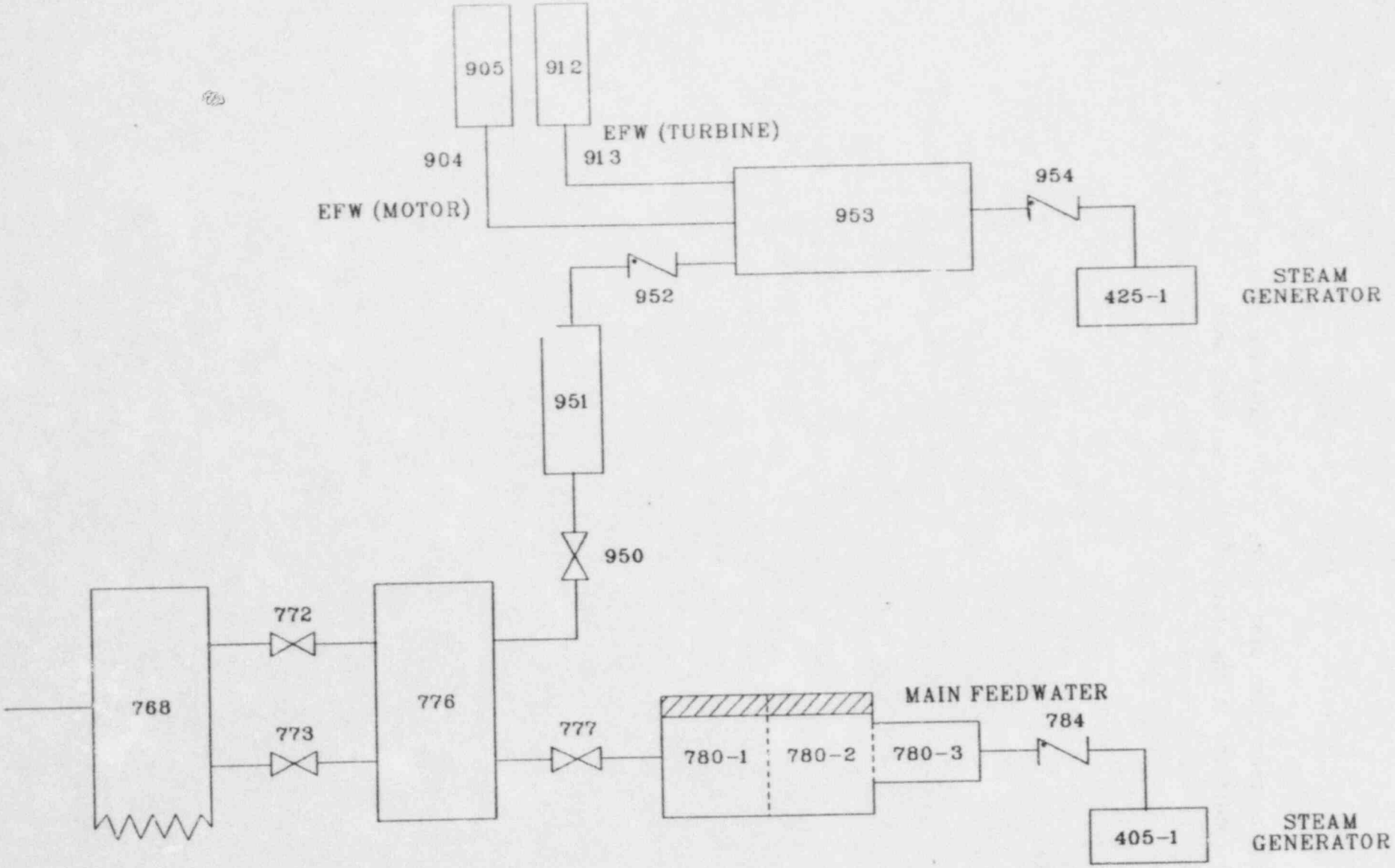

Figure 9. RELAP5 nodalization of the B feedwater header.

2.2 Initial Conditions

Initial conditions used in the RELAP5 model are compared to measured initial conditions at the start of the transient, when available, in Table 1. When measurements were not available, representative initial conditions were obtained from the Final Safety Analysis Report. The measured initial conditions were obtained from strip charts presented in Reference 2. The RELAP5 initial conditions were obtained from a steady state calculation in which the reactor coolant pumps and the feed train were operated by control systems. The calculated values were generally within the expected uncertainty of the actual values, and hence the agreement between calculated and actual initial conditions was excellent.

2.3 Boundary Conditions

The following boundary conditions were assumed for the RELAP5 calculations of the ANO-1 LOSP transient. The assumed boundary conditions were based on information presented in the transient description relative to operator actions, on knowledge of the ANO-1 plant, and on engineering judgement. Engineering judgement was required in determining the boundary conditions because the transient description was not detailed enough to completely specify the transient and because some of the available information was conflicting.

The LOSP caused simultaneous trips of the reactor, the reactor coolant pumps, and the condensate pumps. The turbine stop valves closed 0.1 s after the LOSP. Coastdown of the feedwater flow was calculated by the model.

Core power as a function of time following the reactor trip was represented by tabular values obtained from a separate effects RELAP5 calculation which utilized the code's point kinetics model and accounted for standard[6] and actinide decay heat.

The pressurizer heater and spray control systems were modeled mechanistically. Pressurizer heaters, powered by the diesel generators,

TABLE 1. INITIAL CONDITIONS

	RELAP5	Plant
Core power, MW	2568	2568
Hot leg pressure, MPa (psia)	14.96 (2170)	14.96 (2170)
Hot leg temperature, K (°F)	590 (602.6)	590 (603)
Average reactor coolant temperature, K (°F)	577 (579.1)	578 (580)
Reactor coolant flow, kg/s (lbm/s)	17,600 (38,900)	16,500 (36,500)[a]
Pressurizer level, m (in.)	4.57 (180)	4.57 (180)
Steam generator pressure, MPa (psia)	6.36 (920)	6.31 (915)
Steam generator operating level, %	68	64, 78[b]
Feedwater flow per steam generator, kg/s (lbm/s)	708 (1560)	646, 703 (1425, 1550)[b]
Steam temperature, K (°F)	565 (557)	572 (570)[a]
Feedwater temperature, K (°F)	510 (459)	509 (457)[a]

a. Value obtained from the FSAR because measurement was unavailable.

b. Measured values for both steam generators are presented.

supplied 252 kW of power when the reactor coolant pressure was below 14.8 MPa (2150 psia). The spray valve opened when the reactor coolant pressure exceeded 15.3 MPa (2220 psia) and closed when the pressure dropped below 15.0 MPa (2170 psia). Manual operation of the pressurizer ERV was represented by a control system that opened the valve when the reactor coolant pressure exceeded 16.9 MPa (2450 psia) and closed the valve when the pressure dropped to 16.2 MPa (2350 psia).

For most of the calculations described in this report, HPI was initiated 60 s after the LOSP to simulate a manual action. After 500 s, the HPI flow was multiplied by 0.4 to simulate a manual throttling of HPI. HPI was represented by a flow versus pressure table that was based on the output of two Oconee HPI pumps. Although the capacities of the HPI pumps in ANO-1 and Oconee were nearly identical, the effects of different injection line geometries and the failure of one HPI isolation valve to open on the magnitude of the HPI flow were unknown and were not represented in the model. Furthermore, the exact time HPI was throttled and the amount that the flow was reduced were not known. Consequently, the calculated HPI flow was representative of, but not identical to, the actual flow during the transient. The assumed HPI temperature was 283 K (50°F).

The first pair of safety relief valves on each steam line opened at 7.34 MPa (1065 psia), and the second pair opened at 7.48 MPa (1085 psia). The safety relief valves closed at a pressure 0.38 MPa (55 psi) below where they opened. The RELAP5 safety valve was sized to pass 107 kg/s (235 lbm/s) of dry, saturated steam at 7.34 MPa (1065 psia) for each of the eight safety valves calculated to be open. The ADVs were sized to pass 44 kg/s (97 lbm/s) of dry, saturated steam at 7.03 MPa (1020 psia). The ICS attempted to control turbine header pressure at 7.03 MPa (1020 psia) with the ADVs following the reactor trip. For most of the calculations described in this report, the ADVs were used to control turbine header pressure after 430 s from the LOSP to represent manual dumping of steam. The times when dumping occurred and the amounts of steam actually dumped during the LOSP transient were not known.

ANO-1 has one turbine-driven and one motor-driven EFW pump. Turbine-driven EFW was initiated 15 s after the LOSP. The 15 s delay represented valve sequencing and EFW turbine startup times. Motor-driven EFW was initiated 100 s after the LOSP. The 100 s delay was due to the sequencing logic of the diesel generators. The EFW flow was represented by flow versus pressure tables which were based on the capacity of the Oconee EFW system. Although the capacities of the ANO-1 and Oconee EFW systems are similar, the calculated EFW flow is probably representative of, but not identical to, the actual EFW flow during the LOSP transient. The operators took manual control of EFW when the steam generator operating level reached 50%. A control system was used to represent manual control of the EFW by maintaining the operating level between 40% and 50%. EFW was stopped when the level reached 50% and was restarted when the level dropped to 40%. EFW was throttled to 25% of the maximum capacity of the system after it was restarted. The assumed EFW temperature was 294 K (70°F).

3. RESULTS

The results of four RELAP5 calculations are presented in the following section. Results from a base calculation, which represented the LOSP transient and utilized the model described in Section 2, are presented in Section 3.1. Several sensitivity calculations were performed to investigate the sensitivity of the transient response to operator actions or uncertainty in the assumed boundary conditions. The effects of HPI, EFW, and ADV operation on the transient are described in Sections 3.2. An analysis of how the various conditions simulated in the calculations affected natural circulation and of how natural circulation might be identified in the plant is presented in Section 3.3.

The boundary conditions for the LOSP transient were not known well, primarily because of uncertainties associated with manual operation of the HPI, EFW, ERV, and ADV systems. The exact times of the operator actions and the quantitative effects of the actions on the controlled systems were generally not known. Uncertainties in the boundary conditions resulted in uncertainties in the calculated results. Thus, the calculated results are not expected to overlay the measured data. More emphasis should be placed on the trends of the comparisons between calculated and measured results rather than the magnitude of the differences.

3.1 Base Calculation

A sequence of the significant events occurring in the base calculation is presented in Table 2 to provide an overview of the calculated results. All times are referenced to the time of the LOSP, which was assumed to occur at 0 s. The LOSP caused the reactor, the reactor coolant pumps, and the feedwater condensate pumps to trip. An automatic response of the plant was modeled for the first portion of the transient, including closure of the turbine stop valves, coastdown of the main feedwater, opening and closing of the steam generator safety relief valves, and EFW initiation. HPI was started at 60 s to represent a manual action. The EFW was stopped, representing a manual action, at 430 s, when the steam generator liquid level reached 50% of the operating range. Manual actions were also

TABLE 2. SEQUENCE OF EVENTS

Time(s)	Event
0.0	LOSP; reactor trip; reactor coolant pumps trip; condensate pumps trip
0.1	Turbine stop valves closed
2	Spray valve opened
3	Main feedwater coastdown completed; ADVs opened
4	First pair of steam generator safety relief valves opened
5	Second pair of steam generator safety relief valves opened
9	Spray valve closed
10	Pressurizer heaters on
15	Turbine-driven EFW initiated
17	Second pair of steam generator safety valves closed
28	First pair of steam generator safety valves closed
41	First pair of steam generator safety valves opened
44	First pair of steam generator safety valves closed
60	HPI initiated[a]
100	Motor-driven EFW started
120	Vent valves opened
130	ADVs closed
190	Natural circulation established
390	Pressurizer heaters off
430	EFW stopped,[a] ADVs opened[a]
440	Spray valve opened
500	HPI throttled[a]
660	ERV opened[a]

TABLE 2. (continued)

Time(s)	Event
670	ERV closed[a]
790	EFW restarted[a]
1000	Calculation terminated

a. Represented manual action.

represented at 500 s, when HPI was throttled to slow the pressurizer fill rate, and at 660 s, when the ERV was cycled to limit the reactor coolant pressure. EFW was restarted at 790 s to maintain steam generator liquid level. All the significant events relative to natural circulation had occurred by 1000 s, and the calculation was terminated.

Comparisons between measured plant data and results from the base calculation are presented below. The data available for comparison consisted of reactor coolant pressure, pressurizer liquid level, hot leg and average loop fluid temperatures, and steam generator pressure and level. In addition, cold leg temperature and loop temperature difference were inferred based on a subtraction of the hot leg and average temperatures. However, the uncertainties of the "measured" cold leg temperature and loop temperature difference were larger than the uncertainties in the other data because the uncertainty increases when variables are subtracted.

Calculated and measured reactor coolant pressures are shown in Figure 10. The reactor coolant pressure is directly related to the reactor coolant temperature. When the temperature increases, the liquid in the reactor coolant system expands, compressing the steam space of the pressurizer and increasing the pressure. Conversely, when the temperature decreases, the liquid contracts, expanding the steam space and decreasing the pressure. The response of the reactor coolant temperature will be discussed later. The calculated reactor coolant pressure rapidly increased immediately after the LOSP due to an increase in primary coolant temperature that was caused by a reduction in heat transfer to the steam generators that, in turn, was primarily caused by closing the turbine stop valves. The calculated pressure was limited to a maximum of 15.34 MPa (2225 psia) by the automatic opening of the pressurizer spray valve at 2 s, which caused cold leg fluid to be sprayed into the pressurizer steam space. Following the pressure peak, the calculated reactor coolant pressure decreased rapidly, due to a decreasing reactor coolant temperature, until 60 s when HPI was initiated. The inflow of HPI into the reactor coolant system was sufficient to overcome the depressurization due to cooldown and to begin repressurizing the reactor coolant by increasing the pressurizer level and compressing the steam. The data behaved

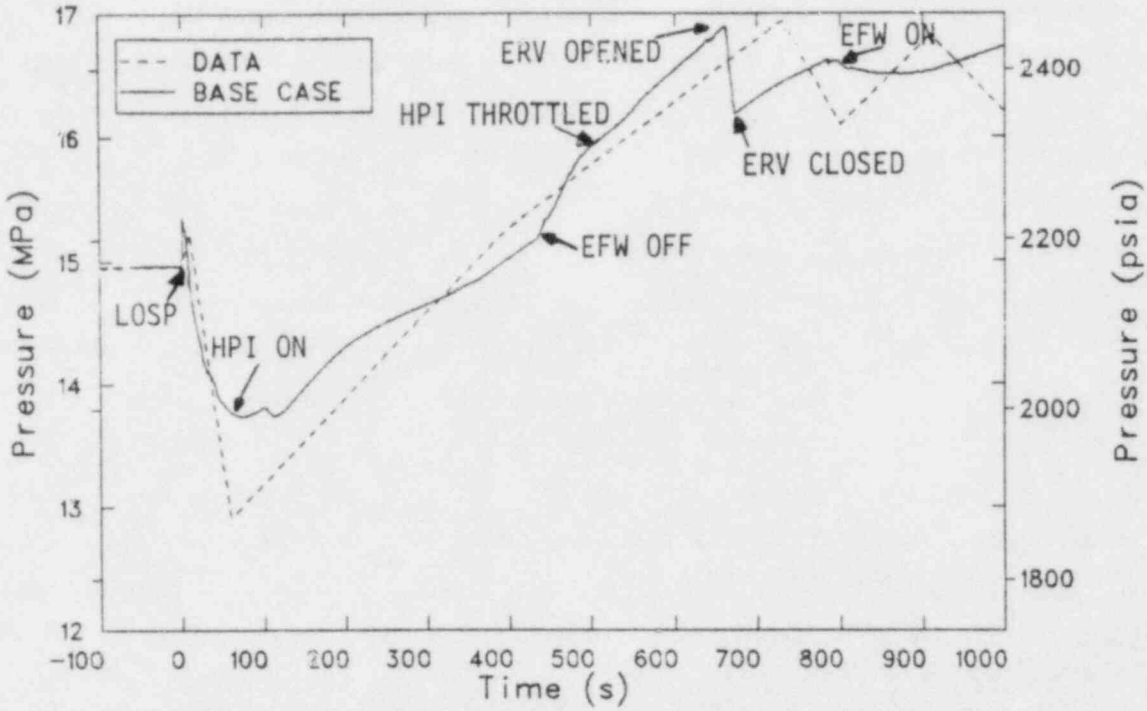

Figure 10. Base case and measured reactor coolant pressures.

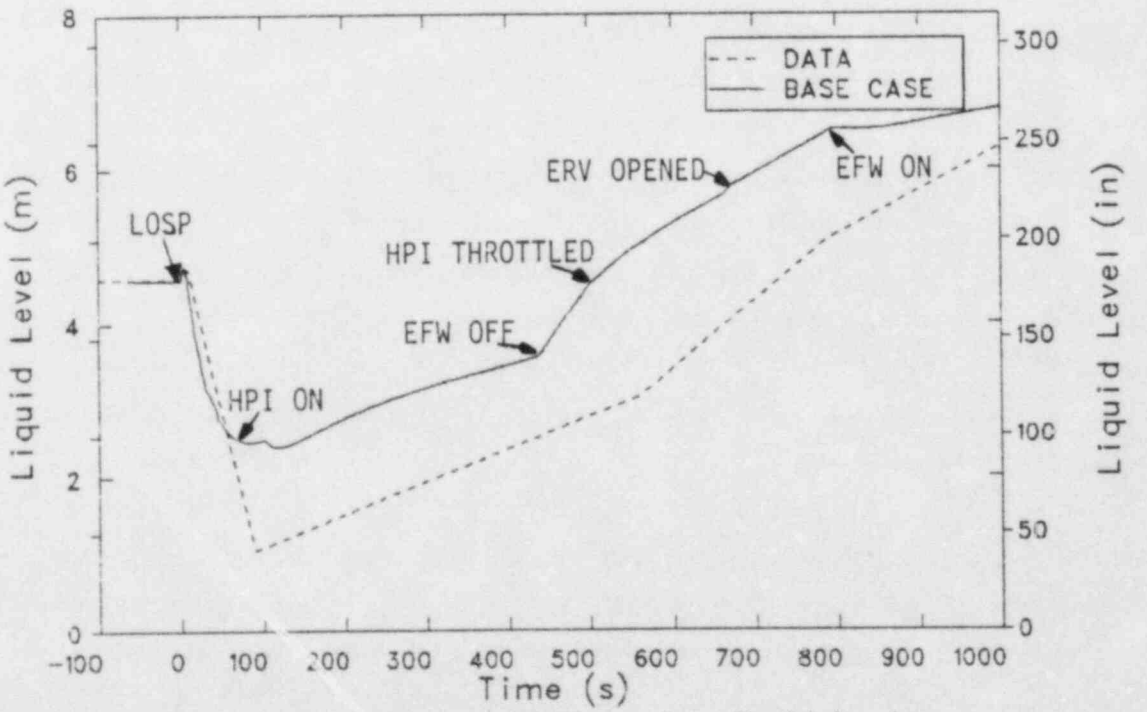

Figure 11. Base case and measured pressurizer liquid levels.

similarly to the calculation for the first 60 s of the transient although the measured minimum pressure was lower than in the calculation. Possible causes for the calculation of a higher minimum pressure than was measured include a higher calculated reactor coolant temperature and the initiation of HPI flow too early in the calculation. The pressure did not decrease enough in either the calculation or the data to cause flashing in the upper head. HPI caused the calculated pressure to increase until 100 s when motor-driven EFW started, causing a slight depressurization due to cooling the steam generator. Between 100 s and 660 s, the measured and calculated pressures increased continuously. The comparison between the calculated and measured results during this time period was very good considering the uncertainty of the data. Three pressure slope changes were calculated between 100 s and 660 s. The first slope change occurred near 200 s and was caused by an increase in the cooldown rate of the hot leg fluid. The pressurization rate increased at 430 s because the cooldown of the reactor coolant stopped when EFW was turned off. The pressurization rate slowed again at 500 s when HPI was throttled. The HPI flow was reduced by 60% at 500 s to simulate a manual action of the operators. The amount of the flow reduction was selected so that the pressurizer ERV opened at about the correct time. The calculated pressure increased to 16.89 MPa (2450 psia) at 660 s, and the ERV opened. Opening the ERV rapidly depressurized the reactor coolant. The reactor coolant pressure dropped to 16.20 MPa (2350 psia) at 670 s, and the ERV closed. The effect of opening and closing the ERV on the pressure was similar in the calculation and the data. Following the closure of the ERV, the calculated pressure increased until 790 s when EFW was restarted. The EFW caused a slight depressurization by cooling the reactor coolant. A similar depressurization was not apparent in the data. The calculated depressurization could have been eliminated by increasing the HPI flow or reducing the EFW flow. The calculated pressure then started increasing again and was near the ERV opening setpoint when the calculation was terminated at 1000 s.

A comparison of calculated and measured pressurizer liquid levels is presented in Figure 11. The calculated level had trends similar to the reactor coolant pressure. The calculated pressurizer liquid level

increased immediately after the LOSP due to a heatup of the reactor coolant and then decreased due to cooldown. The level decrease was halted at 60 s by the initiation of HPI. Changes in the rate of level increase were calculated at 430 s, when EFW was stopped, at 500 s, when HPI was throttled, at 660 s, when the ERV opened, and at 790 s, when EFW was restarted. Although the calculated level was higher than the data after 60 s, the trends of the calculation and data were similar.

A comparison of calculated and measured average cold leg fluid temperatures is presented in Figure 12. The temperatures correspond to a location between the steam generator and the reactor coolant pump. Both calculated and measured temperatures increased following the LOSP as the turbine stop valves closed and the steam generator pressure and temperature increased. The increase in steam generator temperature caused an increase in cold leg temperature because of the thermal communication between the primary and secondary sides of the steam generator. Cycling of the steam generator safety relief valves caused the calculated temperature to decrease, increase, and then decrease again during the first 50 s of the transient. The calculated temperature decreased rapidly after motor-driven EFW was started at 100 s because EFW depressurized and lowered the temperature of the steam generator. The calculated temperature decreased until 430 s, when EFW was turned off. The comparison between calculated and measured temperatures was excellent prior to 430 s, considering the uncertainty in the data. The calculated temperature remained nearly constant after EFW was turned off because of the way the steam generator was controlled, which will be discussed later. The measured temperature was nearly constant after 650 s but was lower than the calculation.

Figure 13 presents a comparison of calculated and measured average hot leg fluid temperatures. The temperatures correspond to a location near the inlet of the steam generator. Both the calculated and measured temperatures decreased rapidly following the LOSP because the core power decreased faster than the core flow, resulting in a smaller temperature rise across the core. The calculated and measured temperatures reached a minimum near 60 s and then began to increase. This temperature increase occurred because the core flow was then decreasing faster than the core

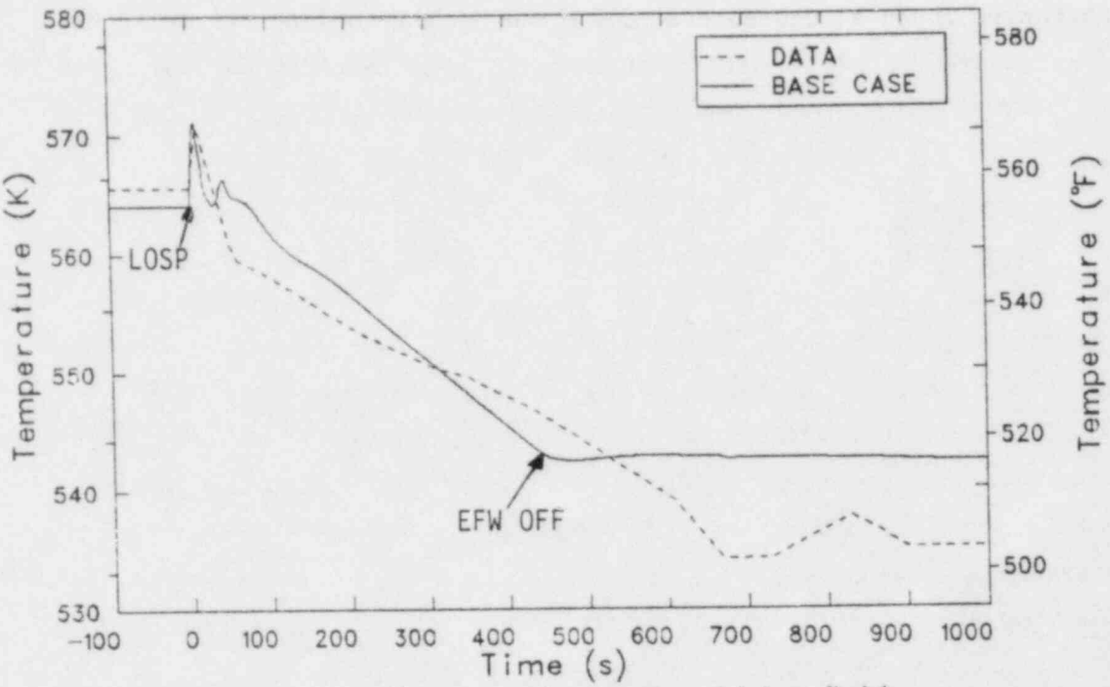

Figure 12. Base case and measured average cold leg fluid temperatures.

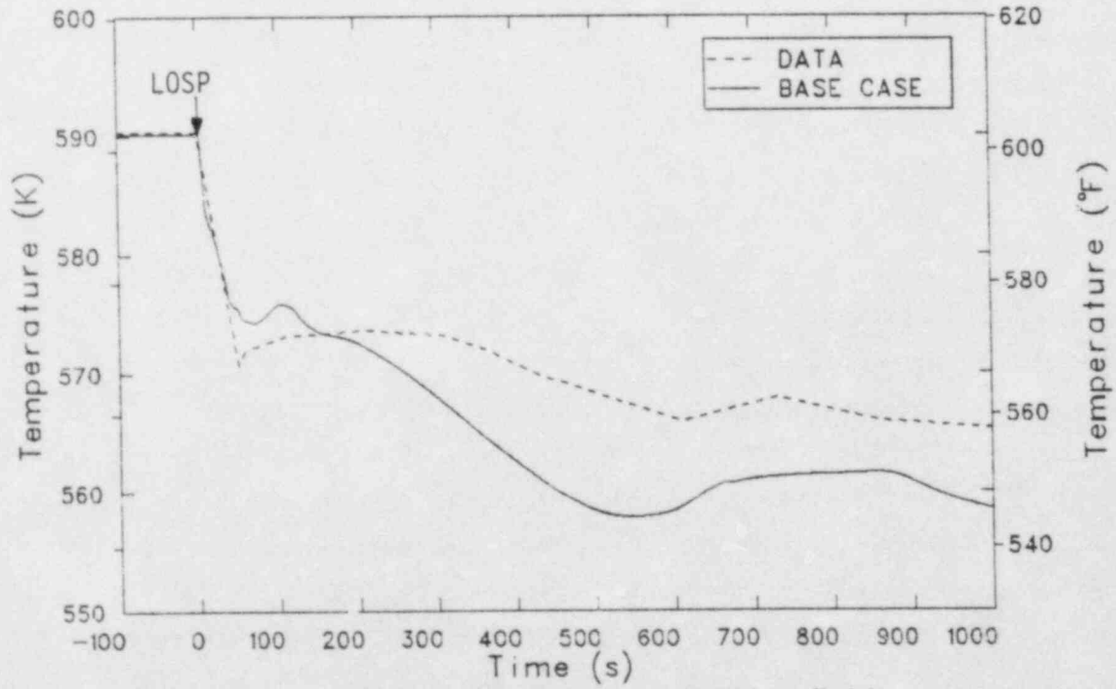

Figure 13. Base case and measured average hot leg fluid temperatures.

power, and the temperature rise across the core increased. The increase in calculated and measured hot leg temperatures was indicative of a transition from forced convection to natural circulation. The calculated hot leg temperature began to decrease at 110 s due to the cooling effect of HPI. HPI was started at 60 s, but because of the time required for the fluid to travel between the HPI injection location and hot leg, the hot leg temperature was not affected until 50 s later. The calculated hot leg temperature began decreasing about 200 s before the measured temperature started decreasing. This may be an indication that either HPI was started earlier in the calculation than in the actual transient or that too much or too cold HPI was assumed. The hot leg temperature cooled down faster in the calculation than in the data between 100 s and 500 s. Since the cooldown rate of the cold leg temperature was calculated reasonably well, as shown in Figure 12, the overprediction of the hot leg temperature cooldown rate can be attributed to calculational problems between the cold and hot legs. The most likely causes of the overprediction of hot leg cooldown rate are too much calculated HPI flow, as discussed previously, or too little flow resistance in the model. A lower than actual flow resistance would cause a higher than actual natural circulation flow, a lower than actual temperature rise across the core, and a lower than actual hot leg temperature. The flow resistance of the reactor coolant system during natural circulation was not known accurately because the flow resistance of the pumps was not known, but was instead based on an extrapolation of available data. The calculated cold leg temperature stopped decreasing at 430 s, when EFW was stopped, but the hot leg temperature continued decreasing until 100 s later because of the time required for the fluid to travel between the cold leg and hot leg. Similarly, the calculated hot leg fluid temperature began increasing about 100 s after HPI was throttled at 500 s. The hot leg temperature stabilized 150 s after HPI was throttled and remained nearly constant until 100 s after EFW was restarted at 790 s. Restarting EFW caused an increase in natural circulation flow that eventually lowered the temperature rise across the core and decreased the hot leg temperature. The trends of the calculated and measured hot leg temperatures were similar after 500 s. Thus, the calculated temperature increase due to throttling HPI and the temperature decrease due to restarting EFW appear to be realistic.

Calculated and measured average reactor coolant temperatures are shown in Figure 14. The temperatures are an average of the cold leg and hot leg temperatures presented previously. The trends of the calculated and measured temperatures were similar. Both the calculation and data show a temperature increase in the first 5 s of the transient. This temperature increase, which was due to an increase in cold leg temperature, caused an increase in reactor pressure and pressurizer level. The average temperature decreased rapidly between 5 s and 30 s, primarily due to the reduction in hot leg temperature following the reactor trip. The calculated cooldown rate increased again near 100 s and 200 s when the effects of the steam generator induced cooldown were felt in the cold leg and the hot leg, respectively. The calculated temperature remained nearly constant after EFW was stopped at 430 s. The good agreement between the calculation and data after 600 s was fortuitous because of compensating errors in the calculation of hot leg and cold leg temperatures.

A comparison of calculated and measured operating liquid levels in the A steam generator is presented in Figure 15. The data for the B steam generator were not available, but the calculated results for the B steam generator were nearly identical to those presented in the figure. Although the calculated level was lower than the data at the time of the LOSP, the calculation was between the measured levels of the two steam generators, as shown in Table 1. The calculated and measured levels decreased rapidly after the LOSP because of coastdown of the feedwater flow and steaming through the safety relief valves and ADVs. The calculated level began increasing when the motor-driven EFW pump started at 100 s, but the increase between 100 s and 230 s was not representative of the actual refill rate because of nodalization effects. The rate of level increase after 230 s was representative of the refill rate in the calculation. The measured level also increased due to EFW. The calculated refill rate was larger than the measured refill rate, but the discrepancy was not large considering the uncertainties in the level data and the EFW flow rate. The calculated level reached 50% at 430 s, at which time EFW was stopped to represent a manual action that occurred during the transient. The calculated level decreased after EFW was stopped due to steaming through the ADVs. A similar decrease in level was measured, although the operators

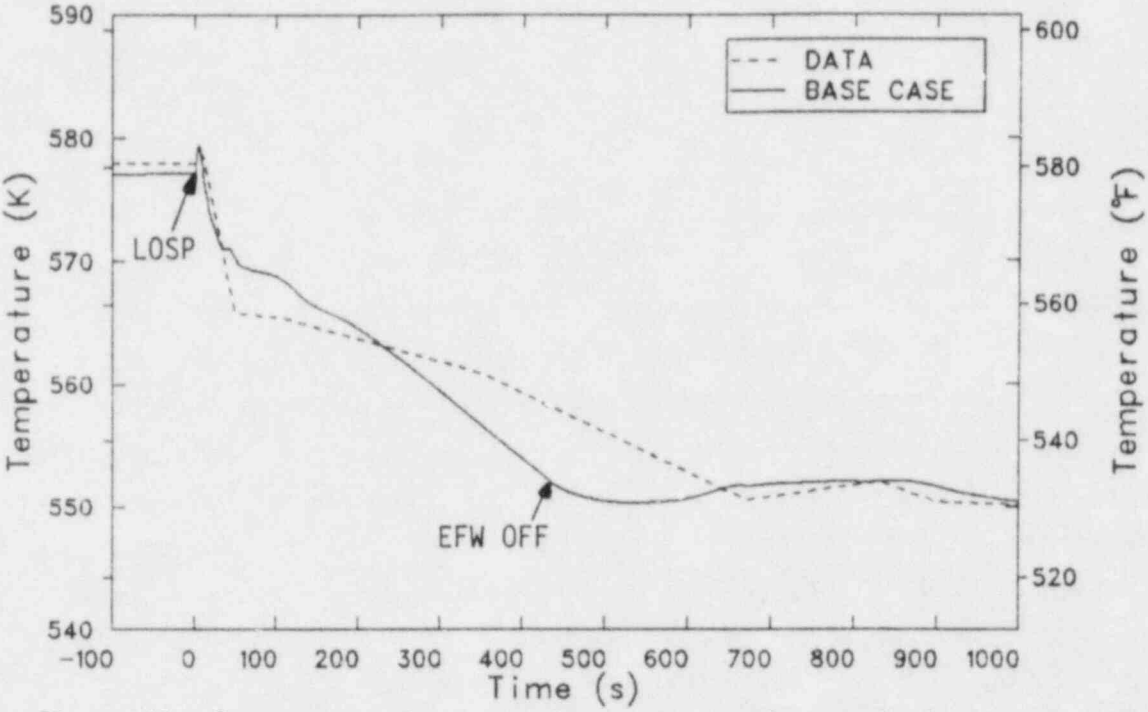

Figure 14. Base case and measured average reactor coolant temperatures.

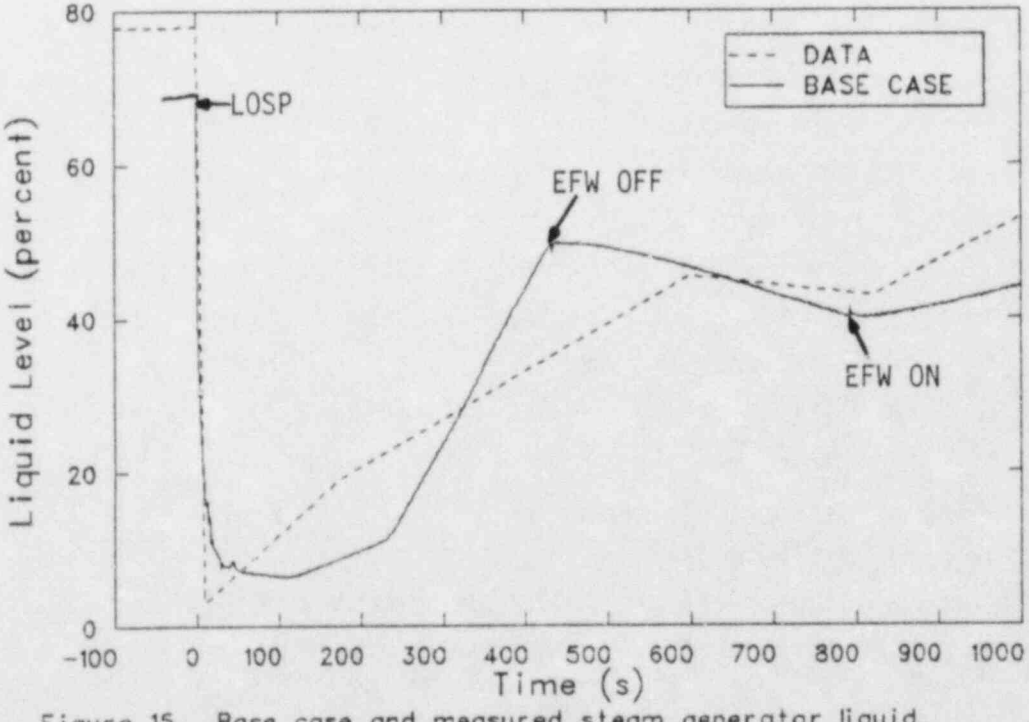

Figure 15. Base case and measured steam generator liquid levels.

probably throttled rather than stopped EFW. The calculated level dropped to 40% at 790 s, EFW was restarted, and the level began to increase. A similar level increase was measured. The EFW was throttled to 25% of the maximum capacity of the system after 790 s in the calculation. A larger EFW flow would have caused a poorer calculation of reactor coolant pressure and pressurizer level.

Calculated and measured steam generator pressures are shown in Figure 16. Only the calculated pressure for the A steam generator is presented because the two steam generators behaved almost identically. The calculated and measured pressures both increased sharply after the LOSP because the turbine stop valves closed and the steam generators were still removing heat from the reactor coolant. The pressure increase in the calculation caused the ADVs to open at 3 s. The ADVs did not have the capacity to limit the pressure rise, and the steam generators continued to pressurize until the safety relief valves opened. The pressure then decreased until 28 s when the safety relief valves closed. The pressure then increased, the safeties reopened, the pressure then decreased, and at 44 s the safeties reclosed. The safety relief valves actually opened during the transient, but the number of open/close cycles could not be determined from the strip chart. The calculated pressure began increasing at 44 s, but the flow through the ADVs and the condensation due to turbine-driven EFW was sufficient to limit the pressure rise and then depressurize the steam generator. The motor-driven EFW pump started at 100 s, and soon afterwards a nearly constant depressurization rate was calculated. After the ADVs closed at 130 s in the calculation, the depressurization was due solely to the condensation caused by EFW. This depressurization of the steam generator by EFW was primarily responsible for the cooldown of the reactor coolant illustrated in Figures 12, 13, and 14. The calculated pressure was higher than the data between 30 s and 100 s, but the calculation and data were generally parallel after 100 s. The calculated depressurization stopped at 430 s when EFW was turned off. The pressure was held constant with the ADVs after 430 s in the calculation. Similarly, the measured pressure remained nearly constant after 530 s. However, the measured pressure stabilized about 0.69 MPa (100 psi) below the calculation. Hand calculations indicated that if the steam flow to the EFW turbine had been

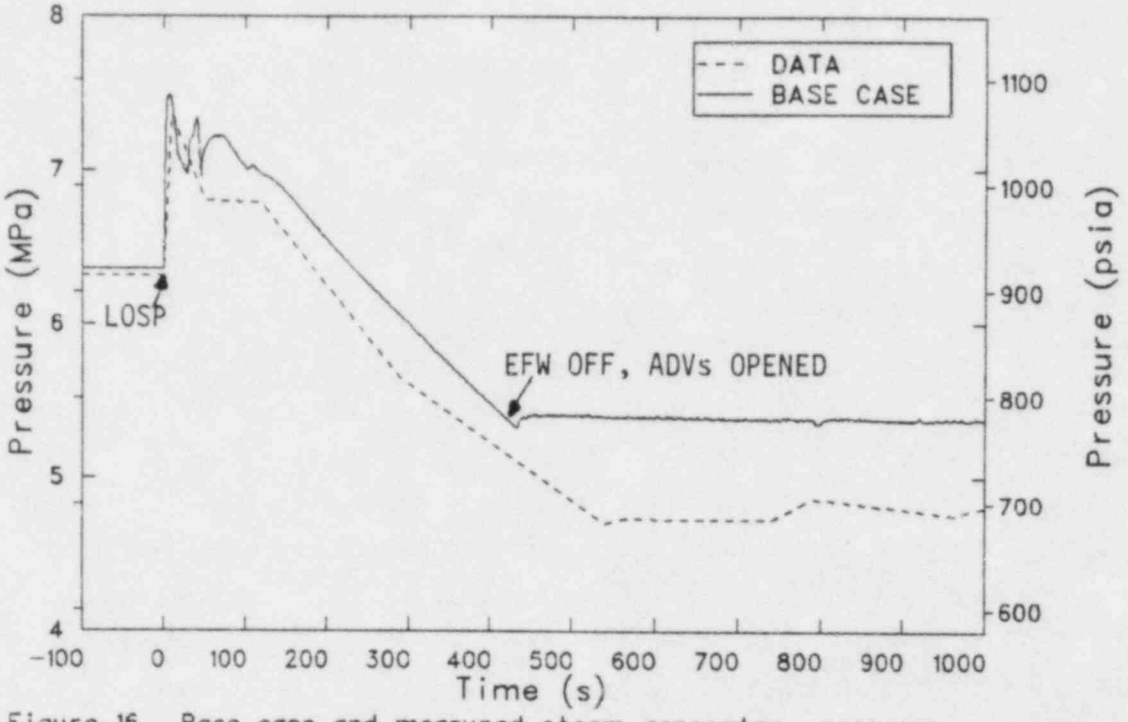

Figure 16. Base case and measured steam generator pressures.

modeled, a more rapid depressurization would have been calculated, and the calculated pressure after 500 s would have been in much better agreement with the data.

3.2 Sensitivity Calculations

Several sensitivity calculations were performed to investigate the sensitivity of the transient response to operator actions or uncertainty in the assumed boundary conditions. The effects of HPI, EFW, and ADV operation on the transient are described in the following section.

A sensitivity calculation was performed to determine the effect of HPI on the LOSP transient. HPI was started at 60 s in the base calculation. The sensitivity calculation was identical to the base calculation except that no HPI was used. The effect of HPI on the reactor coolant pressure and pressurizer level are shown in Figures 17 and 18. In the base calculation, the pressure and level increased after HPI was started. In the sensitivity calculation, the pressure and level continued to decrease after 60 s. The effect of HPI was to recover reactor coolant pressure and pressurizer level following the LOSP.

The effect of HPI on average hot leg temperature is shown in Figure 19. The temperature was slightly higher in the sensitivity calculation between 60 s and 110 s than in the base calculation. The slight temperature difference was due to the pressurizer response. In the base calculation, HPI caused flow into the pressurizer. In the sensitivity calculation, the flow was out of the pressurizer, and the mixing of hot pressurizer fluid with the A loop hot leg fluid caused the average hot leg temperature to be slightly higher than in the base calculation. The calculated temperatures diverged after 110 s. In the base calculation, the temperature decreased at 110 s when the cooling effect of HPI was first felt in the hot leg. In the sensitivity calculation, the temperature did not decrease at 110 s but had a trend similar to the data. An improved calculation of hot leg temperature, compared to the base calculation, could be obtained by delaying the start of HPI, reducing the HPI flow, or increasing the HPI temperature.

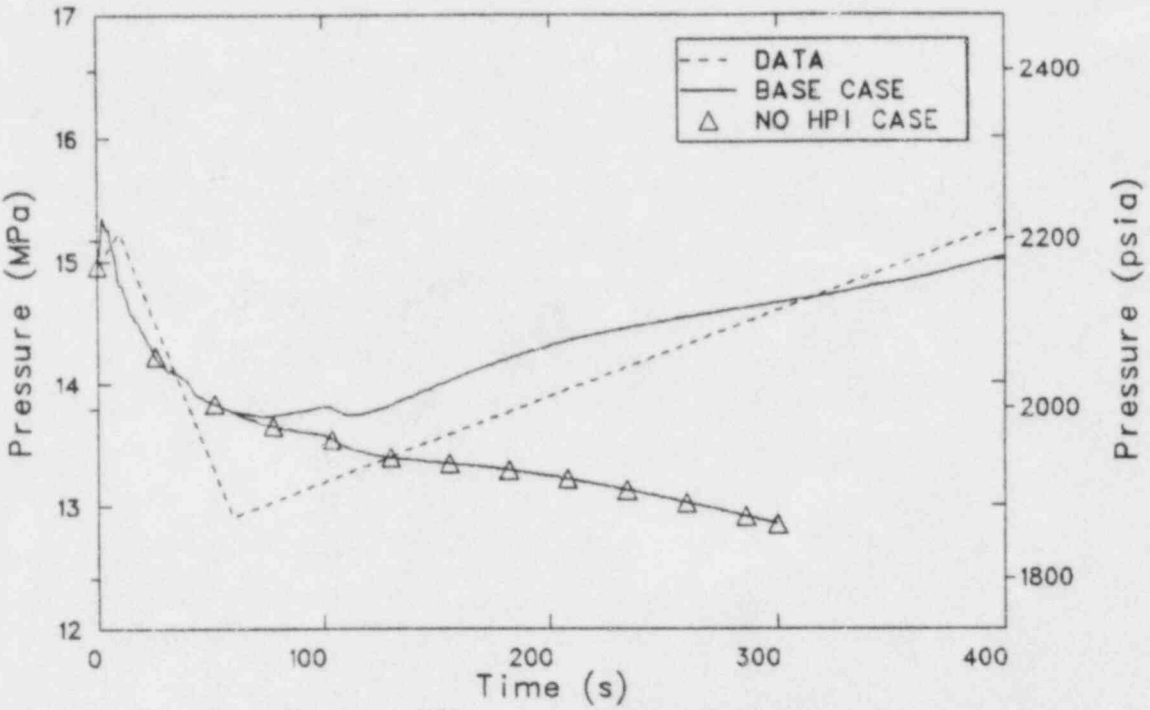

Figure 17. The effect of HPI on reactor coolant pressure.

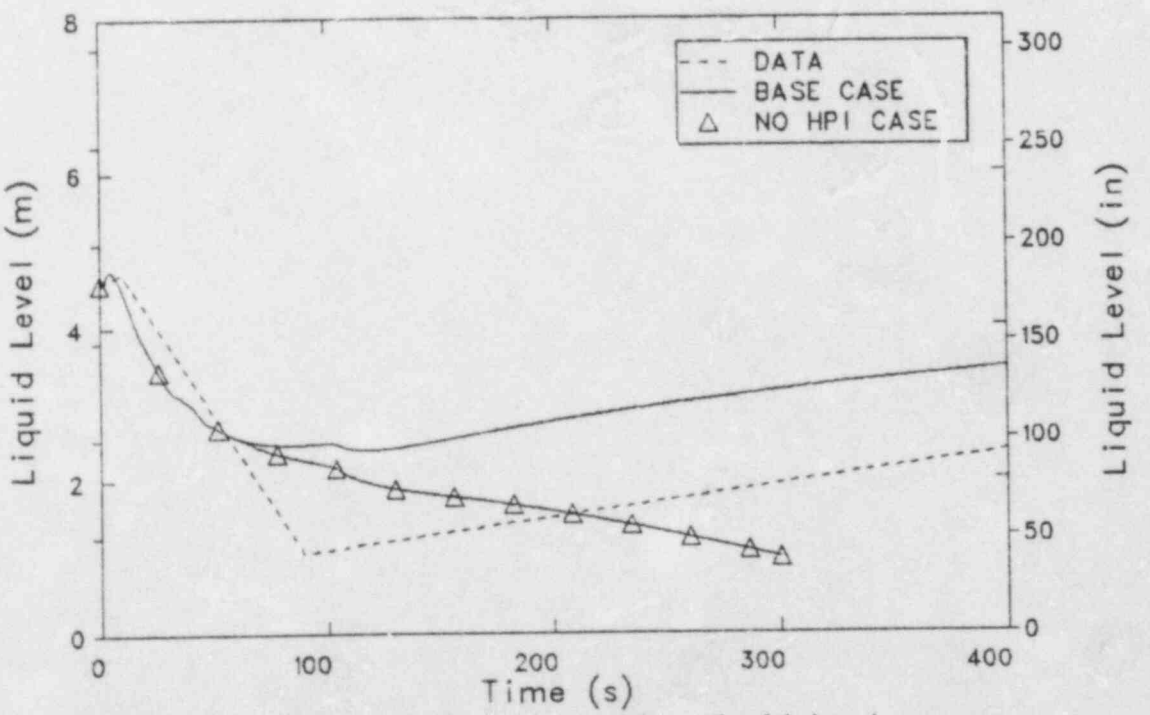

Figure 18. The effect of HPI on pressurizer liquid level.

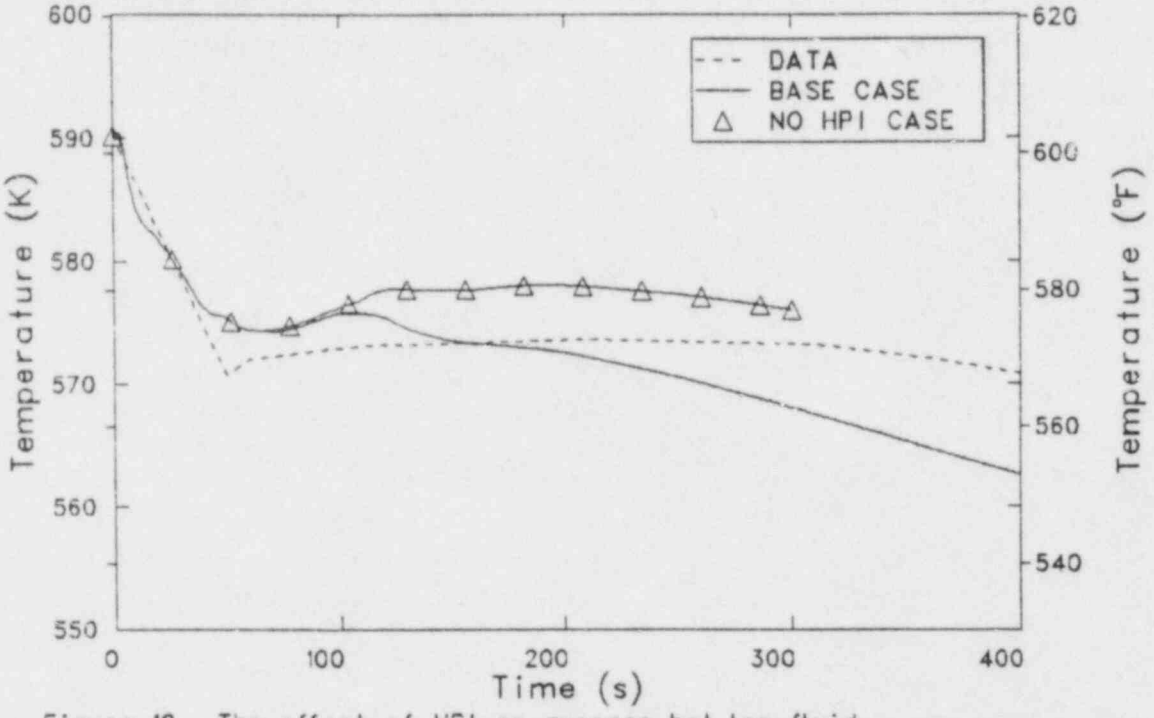

Figure 19. The effect of HPI on average hot leg fluid temperature.

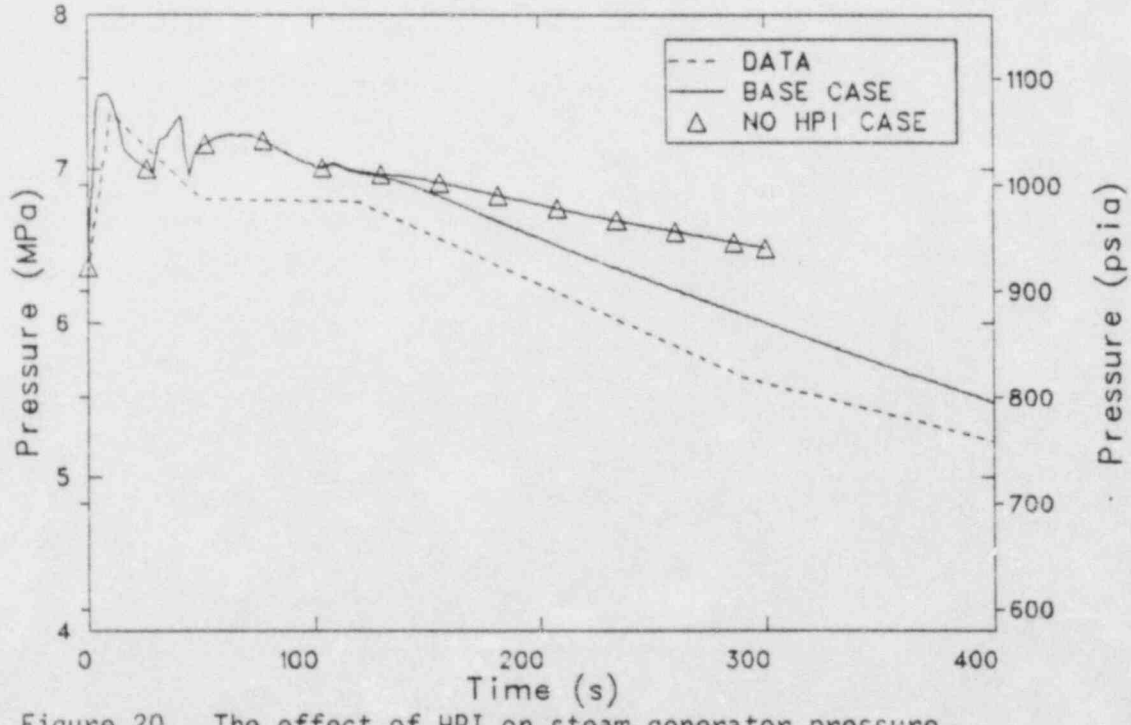

Figure 20. The effect of HPI on steam generator pressure.

HPI significantly affected steam generator pressure, as illustrated by Figure 20. The steam generator pressure decreased more slowly in the sensitivity calculation than in the base calculation because the the hot leg temperature was higher without HPI. The higher hot leg temperature caused more heat transfer to the steam generator and a slower depressurization rate.

A sensitivity calculation was performed to determine the effect of EFW on the transient. In both calculations, turbine-driven EFW started at 15 s, and motor-driven EFW started at 100 s. In the sensitivity calculation, the magnitude of the motor-driven EFW flow was reduced by 50%. The total EFW flow was thus reduced by about 25% after 100 s in the sensitivity calculation. The effect of EFW flow on the steam generator operating level is shown in Figure 21. As expected, the reduced EFW flow in the sensitivity calculation caused a slower refill of the steam generator. The lower EFW flow condensed less steam than in the base calculation, resulting in a slower depressurization of the steam generator, as shown in Figure 22. The slower depressurization of the steam generator in the sensitivity calculation caused a slower reactor cooldown, as illustrated in Figure 23. The slower cooldown caused a more rapid pressurization of the reactor coolant as shown in Figure 24. The differences between the base and sensitivity calculations were significant compared to the differences between the base calculation and the data. Since the EFW boundary conditions were not well known, the comparison of base and sensitivity calculations illustrates that the calculated results are sensitive to the uncertainty in the boundary conditions.

A sensitivity calculation was performed to determine the effect of dumping steam through the ADVs on the LOSP transient. In the base calculation, the ADVs were used to control steam generator pressure after EFW was turned off at 430 s. The sensitivity calculation was identical to the base calculation except that the steam generator was isolated after EFW was stopped and steam was not dumped through the ADVs after EFW was stopped. The effect of dumping steam through the ADVs on steam generator pressure is shown in Figure 25. In the base calculation, the pressure was nearly constant after EFW was stopped. The steam generated by removing

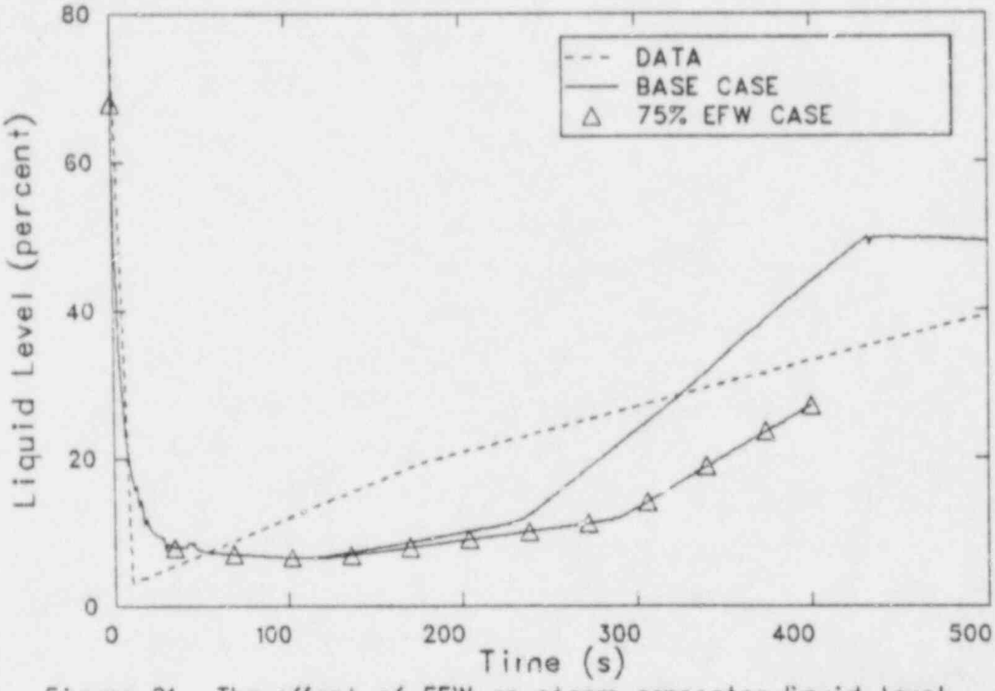

Figure 21. The effect of EFW on steam generator liquid level.

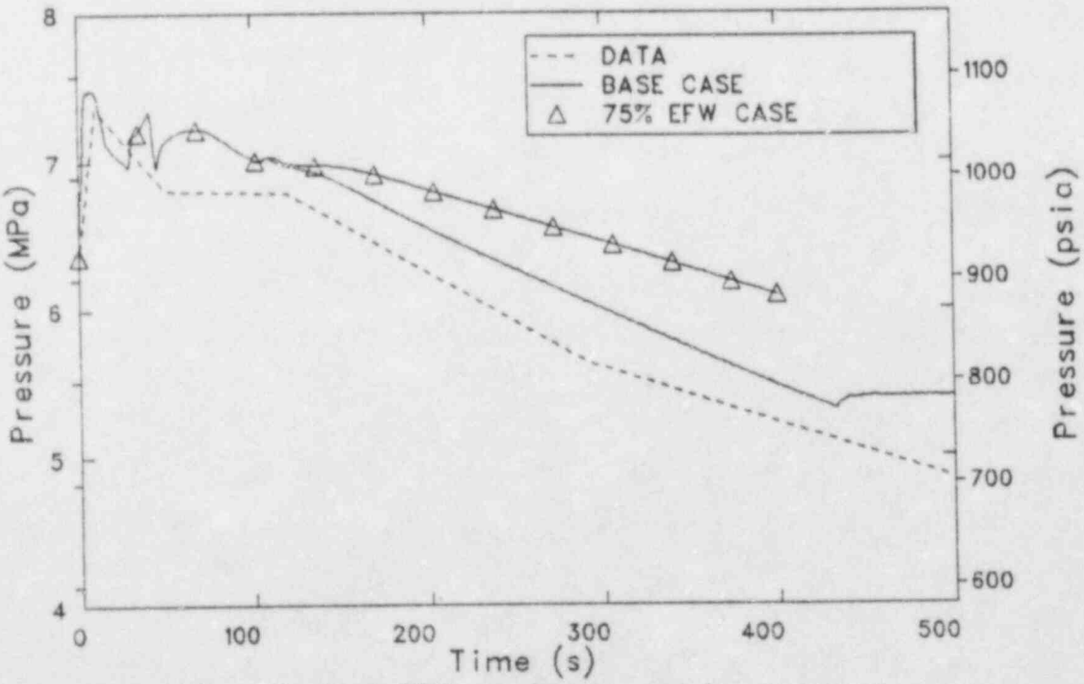

Figure 22. The effect of EFW on steam generator pressure.

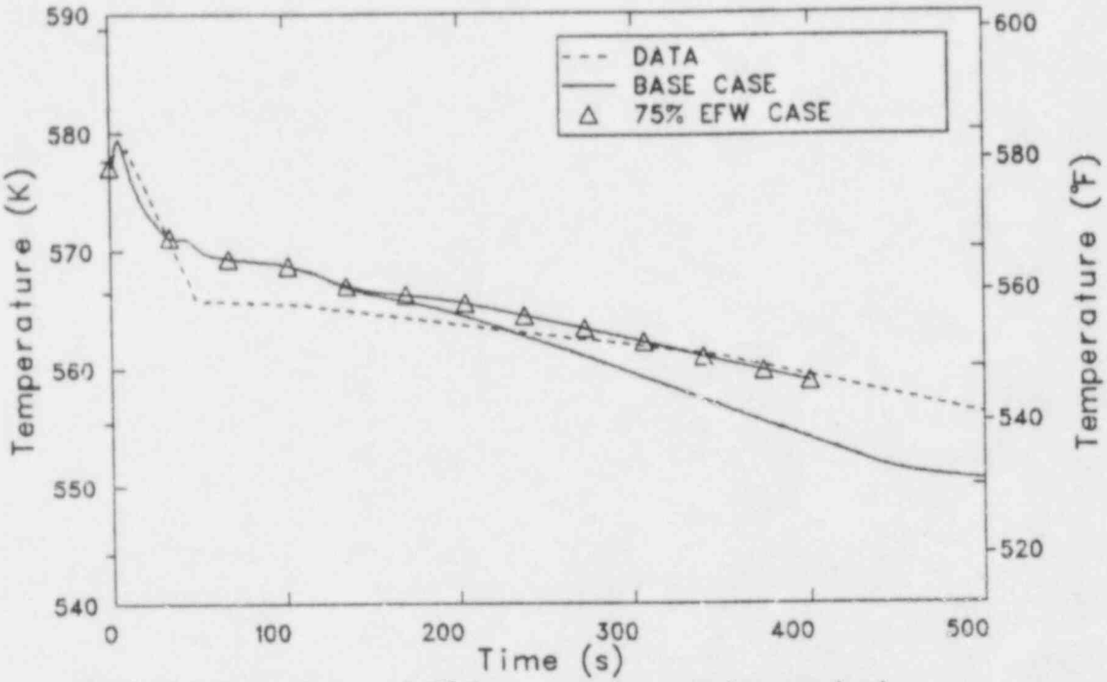

Figure 23. The effect of EFW on average reactor coolant temperature.

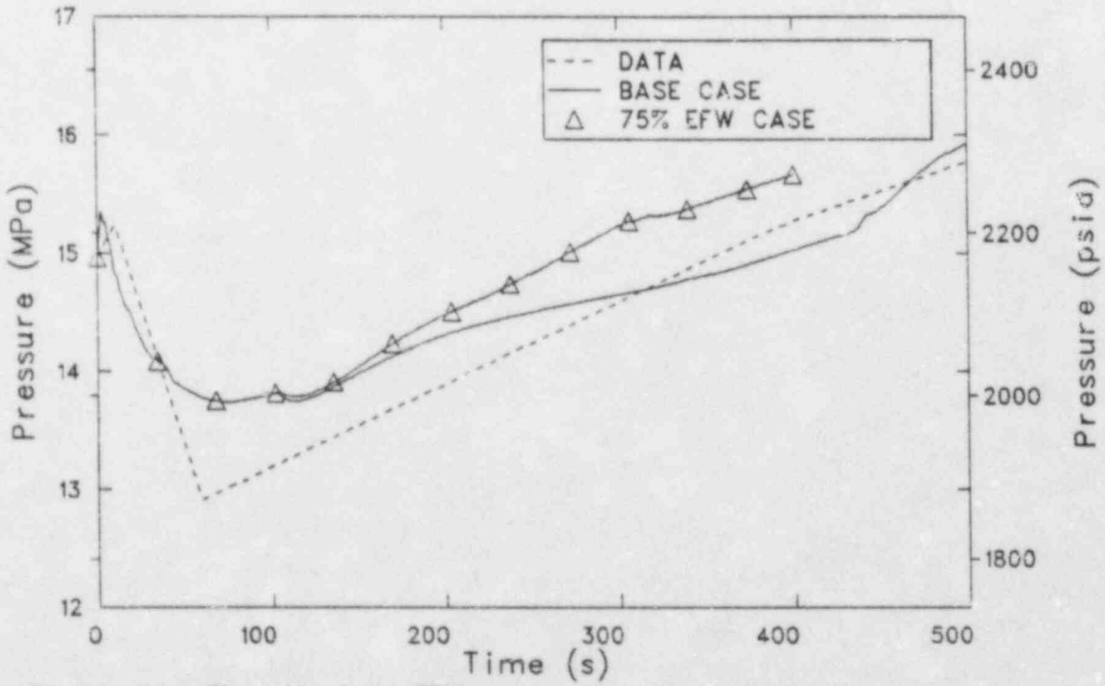

Figure 24. The effect of EFW on reactor coolant pressure.

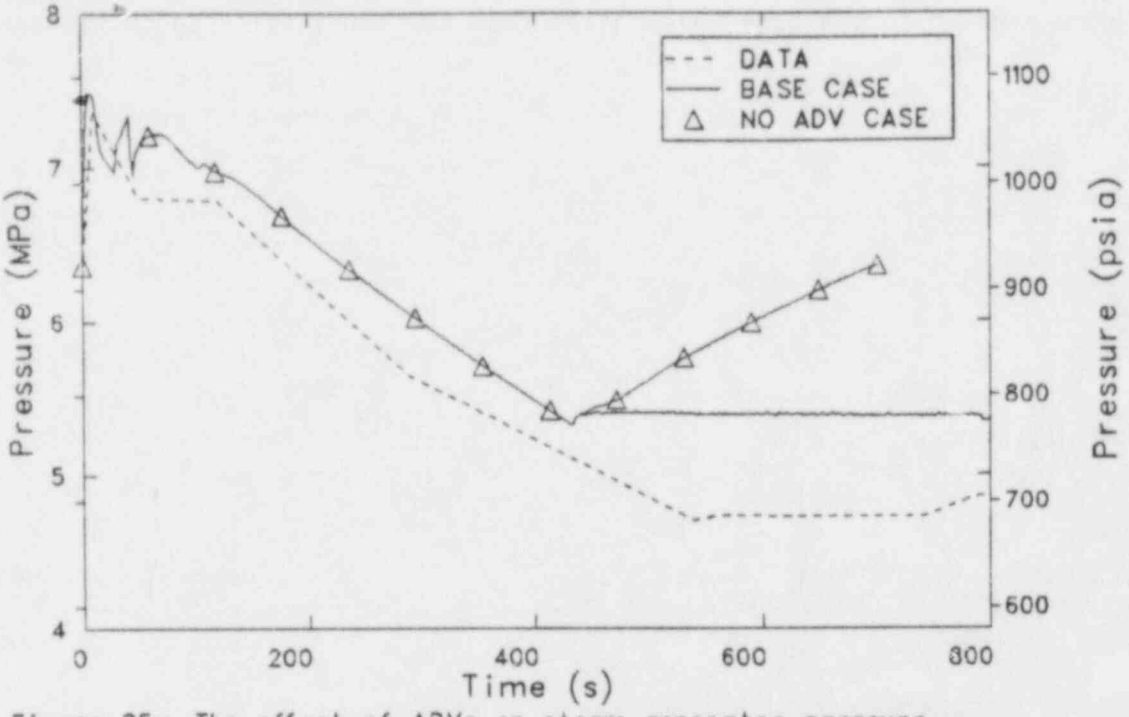

Figure 25. The effect of ADVs on steam generator pressure.

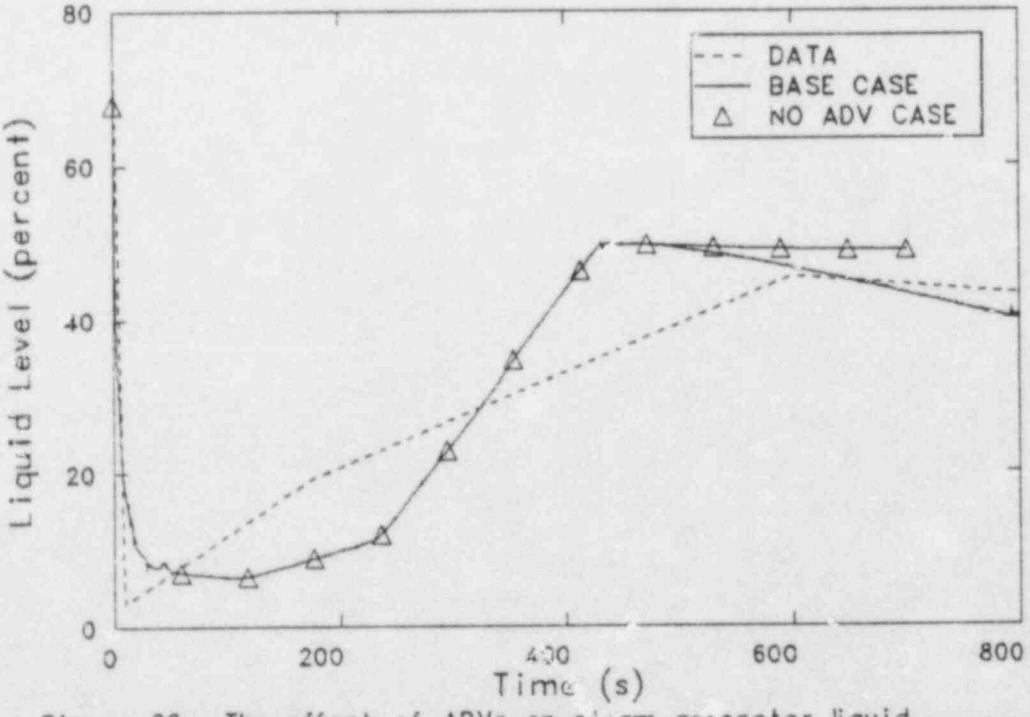

Figure 26. The effect of ADVs on steam generator liquid level.

decay heat from the reactor coolant was relieved thr ugh the ADVs. In the sensitivity calculation, the heat being added to the isolated steam generator caused the pressure to increase. The trends of the data were more similar to the base calculation than the sensitivity calculation.

The effect of dumping steam through the ADVs on the operating liquid level in the steam generator is shown in Figure 26. The liquid level dropped after EFW was turned off in the base calculation because liquid was boiled to steam and then vented through the ADVs. After EFW was turned off in the sensitivity calculation, the mass in the steam generator was constant because the steam generator was isolated. Most of the heat going into the steam generator was stored as sensible heat in the liquid and only a small fraction of the heat boiled liquid to steam. Consequently, the liquid level remained nearly constant in the sensitivity calculation. The trends of the data were more similar to the base calculation than the sensitivity calculation because the measured level decreased after 600 s.

The effect of dumping steam through the ADVs on average reactor coolant temperature is shown in Figure 27. The higher steam generator pressure and temperature in the sensitivity calculation caused an increased reactor coolant temperature compared to the base calculation. Although not shown, the higher steam generator pressure and temperature in the sensitivity calculation also caused higher cold leg temperature, hot leg temperature, reactor coolant pressure, and pressurizer level.

According to Reference 2, steam was not dumped through the ADVs until 600 s after manual control of EFW was taken. Based on the trends of the steam generator pressure and level comparisons shown in Figures 25 and 26, the operators must have dumped steam through the ADVs almost immediately after manual control of EFW was taken.

3.3 Natural Circulation

The hot leg mass flow from the base calculation, normalized by its initial value of 8,820 kg/s, is shown in Figure 28. The mass flow decreased rapidly following the reactor coolant pump trip at 0.0 s. The

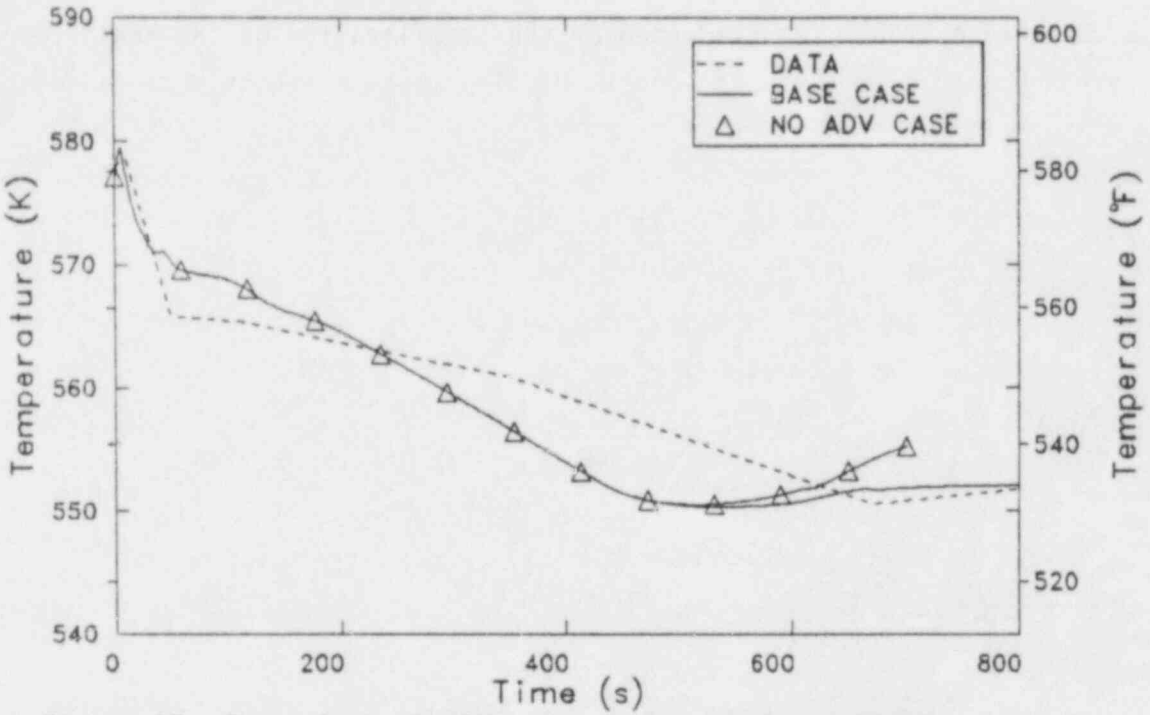

Figure 27. The effect of ADVs on average reactor coolant temperature.

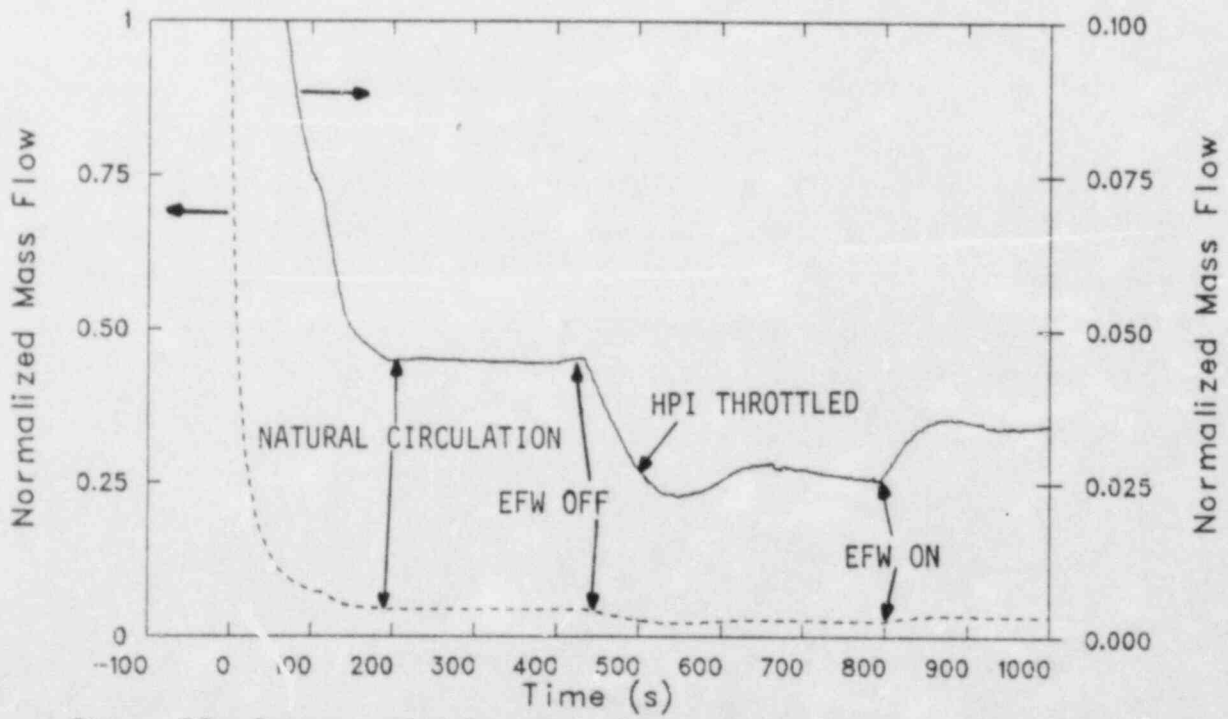

Figure 28. Base case hot leg mass flow rate.

reactor coolant pumps acted as a flow resistance after 110 s, when the pump head became negative. The mass flow continued to decrease until the pump impeller stopped spinning at 190 s. Natural circulation was fully established by 190 s, as evidenced by the stabilization of the mass flow after the pump coastdown was completed. The mass flow rate remained nearly constant until EFW was turned off at 430 s. The EFW affected natural circulation by changing the heat transfer regime within the steam generator. When EFW was on, EFW flowed into the steam space at the top of the steam generator. The EFW then fell through the steam space to the mixture level that was located in the lower half of the steam generator. EFW wetted tubes at the top of steam generator, and most of the heat transfer occurred above the mixture level. The reactor coolant in the upper half of the steam generator tubes was cooled to near cold leg temperature when EFW was on. When EFW was off, the upper half of the steam generator was dry and superheated. Consequently, most of the heat transfer occurred below the mixture level, and the reactor coolant in the upper half of the steam generator was nearly at hot leg temperature. The temperature of the reactor coolant in the upper half of the steam generator increased when EFW was turned off at 430 s. The difference in temperature between the reactor coolant in the hot leg and the upper half of the steam generator contributed to the gravitational head that caused natural circulation flow. Thus, the temperature increase in the upper half of the steam generator reduced the driving head for natural circulation flow, and the mass flow decreased after EFW was turned off. The hot leg mass flow increased shortly after HPI was throttled at 500 s. The hot leg temperature increased after HPI was throttled while the cold leg temperature was held constant by the ADVs, as shown in Figures 12 and 13. The increased temperature difference between the hot and cold leg temperatures due to throttling HPI caused an increase in natural circulation flow. The mass flow increased again when EFW was turned back on at 790 s. The EFW flow increased the heat transfer above the mixture level in the steam generator, reducing the temperature of the reactor coolant in the upper half of the steam generator, and increased the gravitational driving head for natural circulation.

The calculated effect of EFW on natural circulation flow may be too large. In the calculation, EFW was distributed uniformly, in a radial sense, and wetted all the steam generator tubes. However, recent data[7] indicate that only a limited number of tubes are actually wetted. Since RELAP5 may calculate that too many tubes are wetted, it may also calculate too much heat transfer above the mixture level. Consequently, the effect of EFW on natural circulation flow may be overstated by the calculation, although the calculated trends are probably correct.

Mass flow rates below 5% of normal operating flow, as were calculated in natural circulation, are generally not within the measurement range of plant flow instrumentation. Other measurements need to be examined to verify the presence of natural circulation. Measurements which have the potential to verify natural circulation include a combination of steam generator and cold leg temperature measurements. Steam generator and cold leg temperatures from the base calculation and data are shown in Figure 29. The steam generator temperatures correspond to saturation temperature based on the steam generator pressures shown in Figure 16. The cold leg temperatures, shown previously in Figure 12, were taken upstream of the HPI injection location. A comparison of calculated steam generator and cold leg temperatures shows that the two temperatures were closely coupled during natural circulation. The flow rate was low enough that the reactor coolant was cooled nearly to secondary temperature by the time it left the steam generator. The difference between calculated temperatures was generally less than 2 K (3.6°F) during natural circulation. The difference between measured steam generator and cold leg temperatures during natural circulation was also small, considering the uncertainty in the digitized data. Based on the information presented in Figure 29, the steam generator and cold leg temperatures should be closely coupled if natural circulation is occurring. The coupling between temperatures is an indication of natural circulation, but it is not a sufficient condition for natural circulation.

The difference between hot and cold leg temperatures is another indication of loop flow. The loop temperature differences from the base calculation and the data are shown in Figure 30. The loop temperature

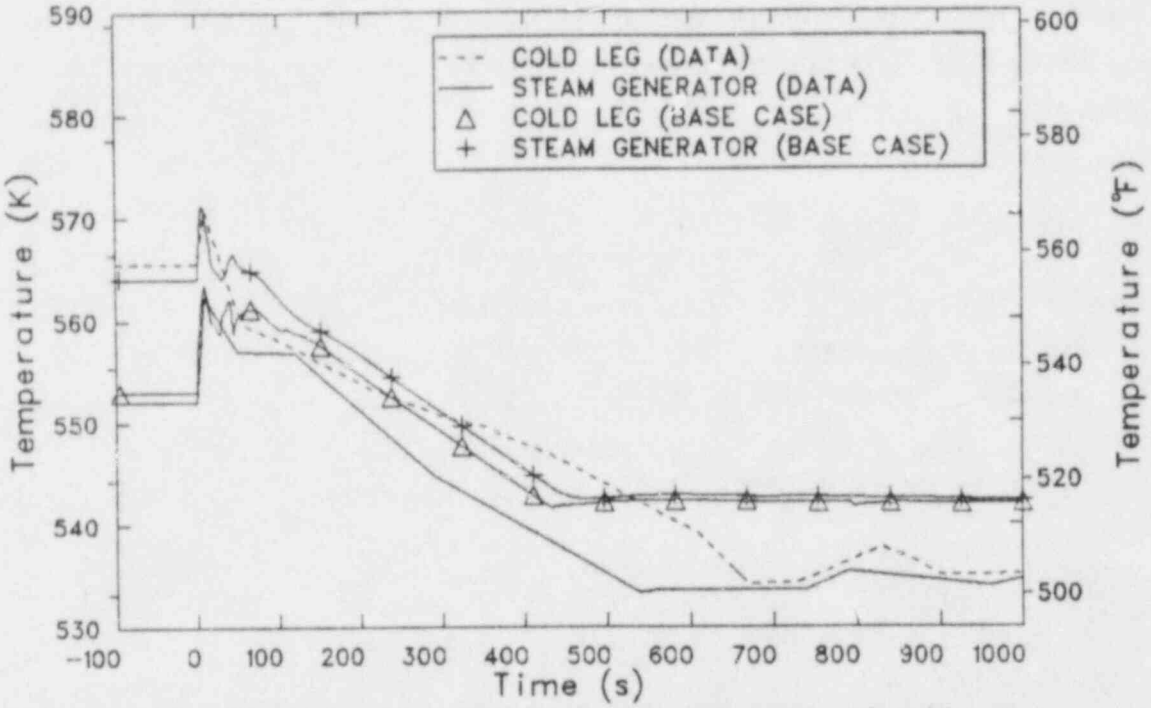

Figure 29. Comparison between base case and measured cold leg and steam generator temperatures.

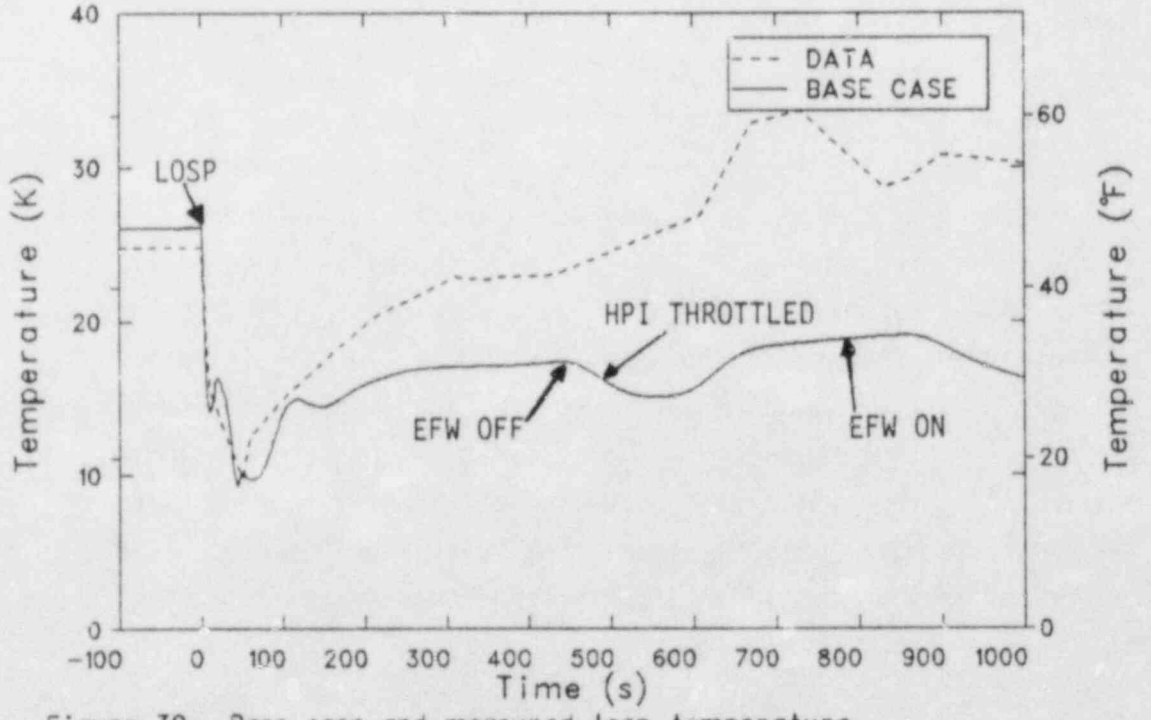

Figure 30. Base case and measured loop temperature differences.

difference was obtained by subtracting the average cold leg temperature, shown in Figure 12, from the average hot leg temperature, shown in Figure 13. The calculated temperature difference decreased rapidly following the LOSP because the core power decreased faster than the reactor coolant flow. The temperature difference began increasing near 60 s as the flow coastdown continued and the core power decay slowed. This increase in temperature difference was associated with the transition from forced convection to natural circulation. The calculated temperature difference decreased slightly at 110 s, when the cooling effect of HPI was first felt in the hot legs. The calculated temperature difference then increased slowly until the coastdown of the reactor coolant pumps was finished and natural circulation was established at 190 s. The temperature difference stabilized shortly after natural circulation was established and remained nearly constant until 430 s, when EFW was stopped and the ADVs were used to control steam generator pressure. The temperature difference then decreased because the cold leg temperature was held constant by the ADVs while the hot leg temperature continued to decrease due to transit time effects. At 430 s, the transit time for the fluid to travel between the cold leg and the hot leg was 140 s. The hot leg temperature and loop temperature difference would have stabilized at 430 + 140 = 570 s in the absence of flow changes. However, the temperature difference actually stabilized earlier, about 530 s, because the natural circulation flow decreased and the temperature difference across the core increased when EFW was stopped. Throttling HPI at 500 s caused an increase in temperature difference, although the effect was not felt until 100 s later in the hot leg. Similarly, the temperature difference decreased about 100 s after EFW was restarted at 790 s. The decrease in temperature difference was caused by the corresponding increase in natural circulation flow shown in Figure 28. An apparent contradiction in the effect of EFW on loop temperature difference is shown in Figure 30. The calculated loop temperature difference decreased when EFW was stopped and then decreased again when EFW was restarted. The temperature decrease caused by stopping EFW was due to transit time effects and the transition from a rapid cooldown to a nearly steady state. The temperature decrease caused by restarting EFW was due to an increase in natural circulation flow and a

change from one steady state to another. Thus, the effect of EFW on loop temperature difference varies depending on whether the reactor coolant system is undergoing a cooldown or is near steady state.

A comparison of calculated and measured loop temperature differences, shown in Figure 30, reveals that the trends of the two were similar although the calculated temperature difference was smaller than the data after 100 s. The calculated temperature difference was too low because the calculated hot leg temperature, shown in Figure 13, was too low. The cause of the underprediction of temperature difference was probably a combination of too much HPI flow and too little loop flow resistance in the calculation. The calculation shows that manual actions relative to HPI and EFW increased or decreased the loop temperature difference. Similar increases and decreases appear in the data. The calculation and data both indicate that the loop temperature difference responds, after a time delay, to actions affecting the steam generator.

The effect of throttling HPI on hot leg mass flow in the base calculation was discussed previously. The effect of turning on HPI is illustrated in Figures 31 and 32, which compare results from the base calculation and the HPI sensitivity calculation. In the base calculation, HPI was started at 60 s, while in the sensitivity calculation, HPI was not used. The cooling effect of HPI lowered the hot leg temperature relative to the cold leg temperature. Consequently, the loop temperature difference was higher when HPI was not used, as shown in Figure 31. The higher temperature difference in the sensitivity calculation increased the driving head for natural circulation and caused a slightly higher hot leg mass flow, as shown in Figure 32. The flow was about 6% higher in the sensitivity calculation once natural circulation was established.

The effects of EFW flow on loop temperature difference and hot leg mass flow are shown in Figures 33 and 34, which compare results from the base and EFW sensitivity calculations. In the sensitivity calculation, the EFW flow was reduced by 25% after 100 s. The reduced EFW flow in the sensitivity calculation caused a less rapid depressurization of the steam generator and a less rapid cooldown of the reactor coolant. The cooldown

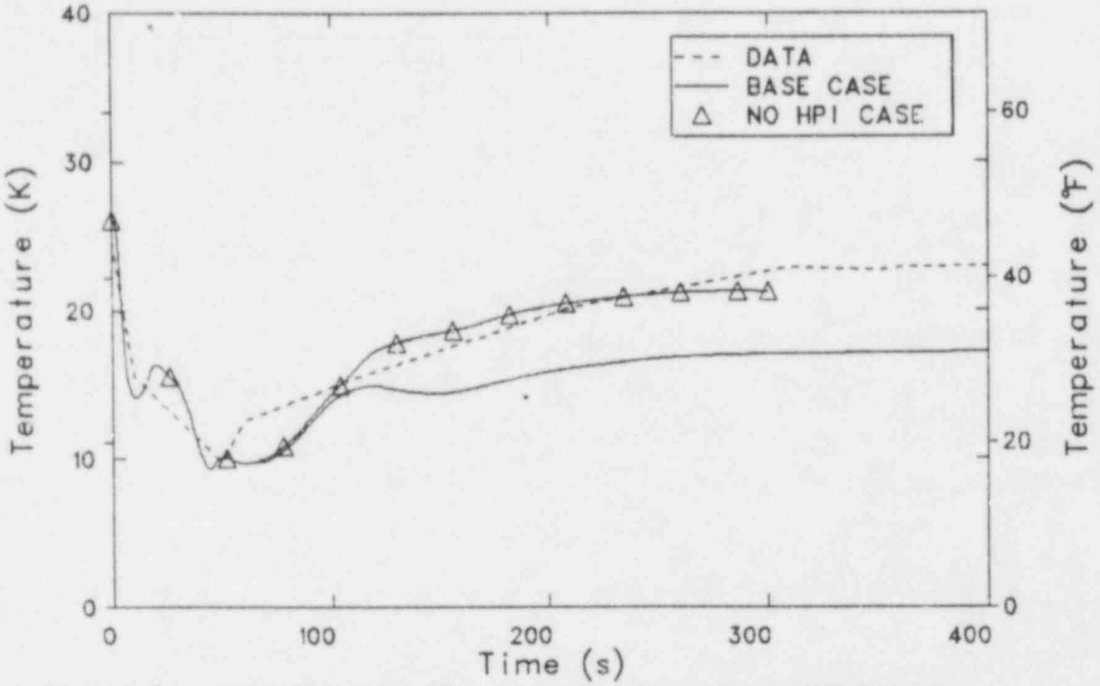

Figure 31. The effect of HPI on loop temperature difference.

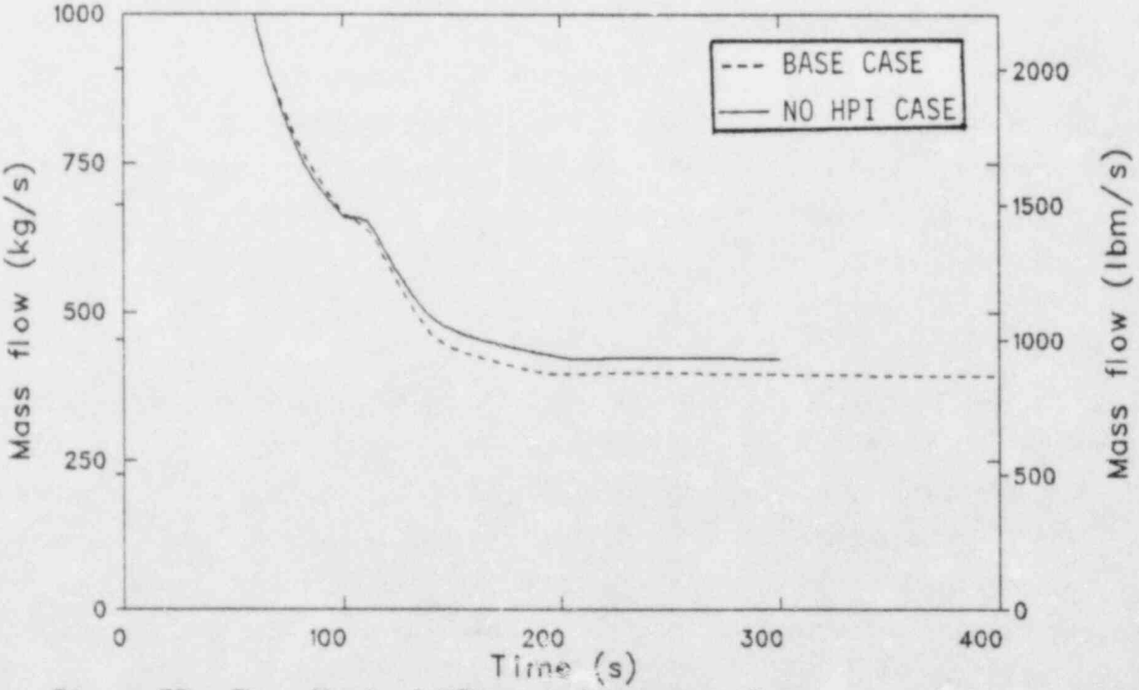

Figure 32. The effect of HPI on hot leg mass flow.

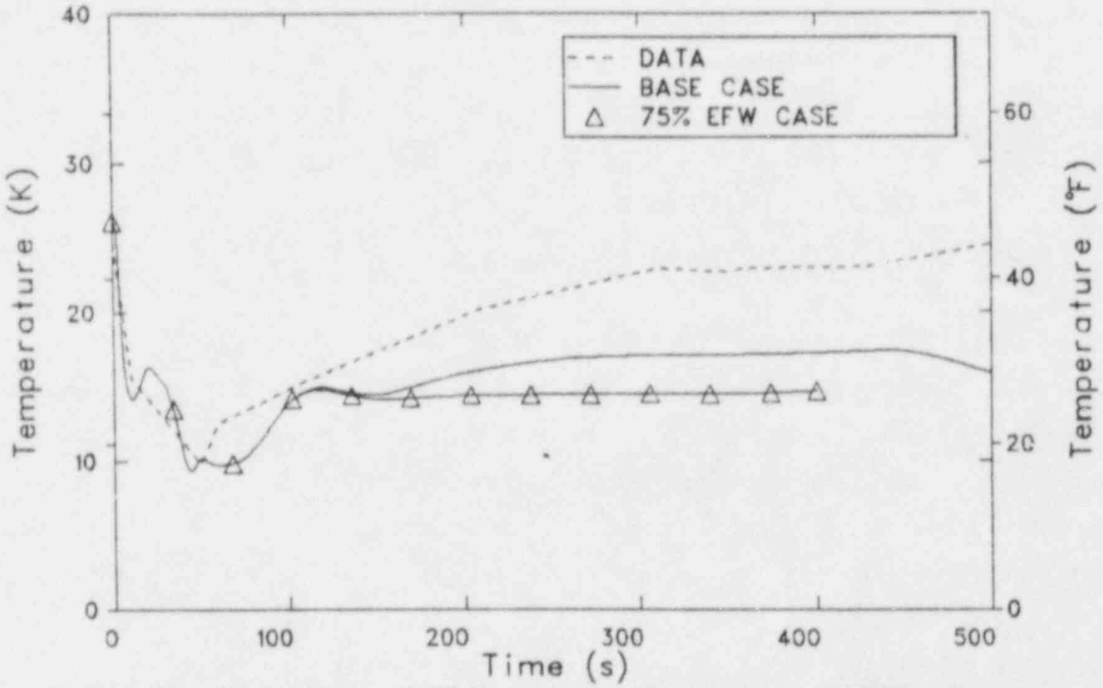

Figure 33. The effect of EFW on loop temperature difference.

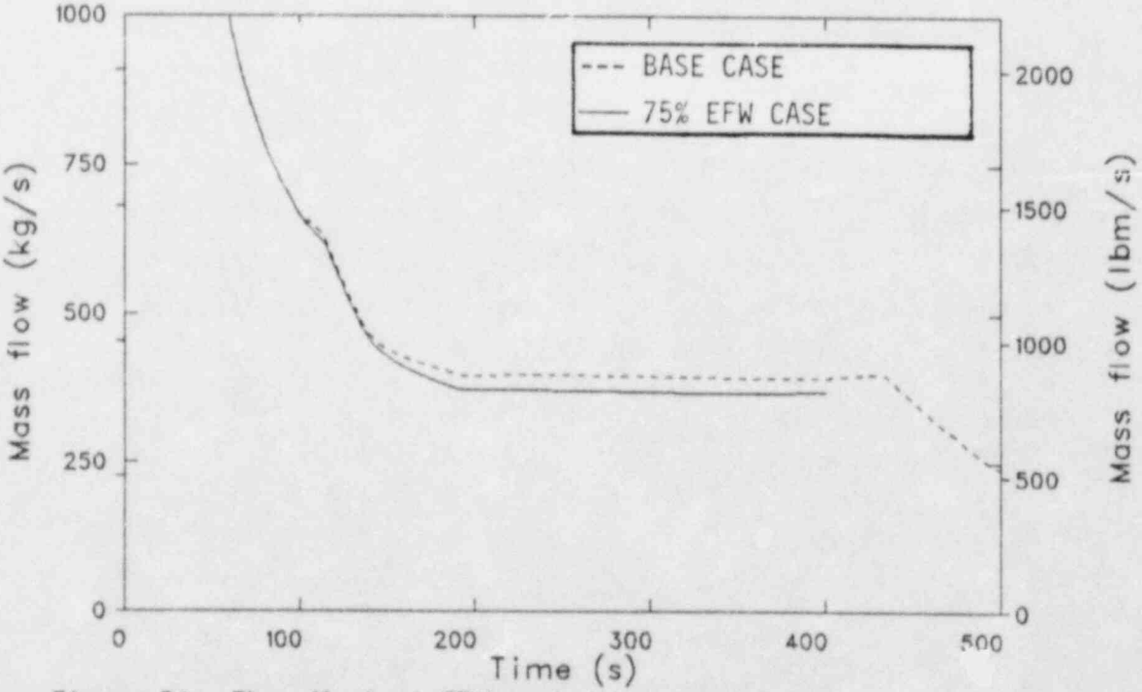

Figure 34. The effect of EFW on hot leg mass flow.

rate affected the loop temperature difference because of a transient effect. By the time a particle of fluid traveled from the cold leg to the hot leg, the cold leg temperature had decreased, causing a larger temperature difference than would have existed in the absence of a cooldown. The less rapid cooldown rate in the sensitivity calculation caused a slower decrease in cold leg temperature and a smaller loop temperature difference than in the base calculation. The smaller loop temperature difference in the sensitivity calculation resulted in a slightly lower natural circulation flow, as shown in Figure 34.

The effects of using the ADVs on loop temperature difference and hot leg mass flow are shown in Figures 35 and 36, which compare results from the base calculation and the ADV sensitivity calculation. In the base calculation, the ADVs were opened at 430 s to control steam generator pressure after 430 s. In the sensitivity calculation the ADVs were not opened. The steam generators repressurized after 430 s, causing a heatup of the reactor coolant, in the sensitivity calculation. The heatup of the reactor coolant lowered the loop temperature difference, shown in Figure 35. The lower loop temperature difference caused a slightly lower natural circulation mass flow, shown in Figure 36. The effect of a heatup of the reactor coolant on natural circulation was similar to the effect of a reduced cooldown rate.

A sensitivity calculation was performed to determine the effect of cycling the ERV on natural circulation. In the base calculation, the ERV opened at 660 s and closed 10 s later. In the sensitivity calculation, the ERV did not open. The hot leg mass flow was almost identical in the two calculations. Thus, natural circulation was not significantly affected by cycling the ERV. The ERV was not open long enough to affect loop temperature distribution and natural circulation flow.

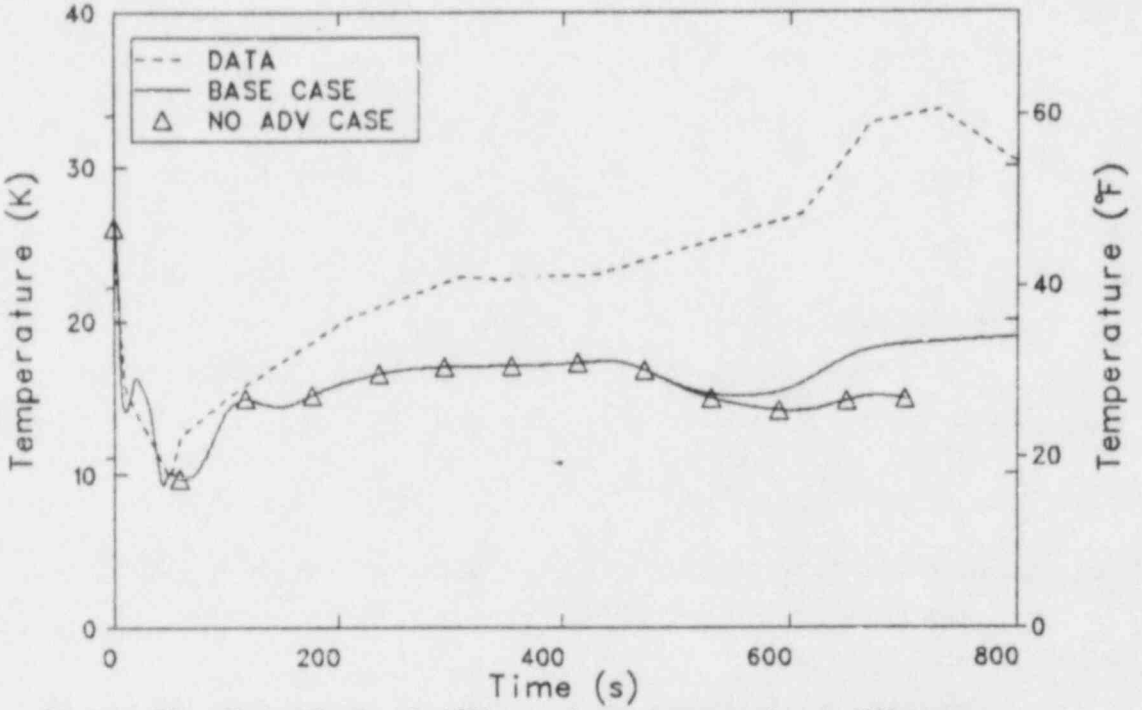

Figure 35. The effect of ADVs on loop temperature difference.

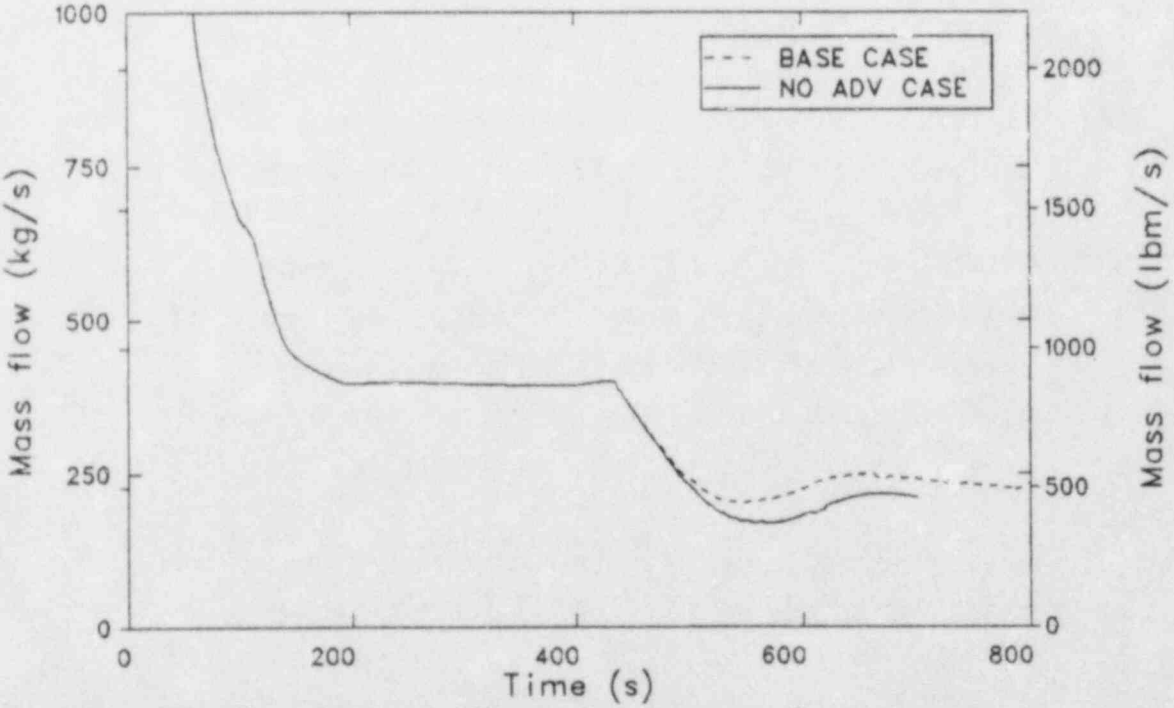

Figure 36. The effect of ADVs on hot leg mass flow.

4. CONCLUSIONS

Conclusions derived from the analysis of the April 7, 1980 LOSP transient at ANO-1 are presented below.

1. All the significant operator actions taken during the LOSP transient were reported in the transient description.

   The trends of the transient were reproduced in the base calculation, which represented the major operator actions listed in the transient description (Reference 2). If other significant manual actions had occurred, the trends of the calculation would have been deficient.

2. The reactor operators opened the ADVs earlier than was reported in the transient description.

   According to the transient description, the ADVs were opened 300 s after manual control of the EFW was taken. However, as shown in Figures 25 and 26, the trends of the steam generator pressure and liquid level were more accurately calculated when manual control of the EFW and ADVs were taken at the same time.

3. The manual initiation of HPI had a major impact on the thermal-hydraulic response of the reactor coolant system during the transient.

   HPI pressurized the reactor coolant and increased the liquid level in the pressurizer, as shown by Figures 17 and 18. HPI also decreased the hot leg temperature and increased the reactor cooldown rate as shown in Figures 19 and 20.

4. The thermal-hydraulic response of the reactor coolant system was sensitive to the behavior of the steam generator.

The cold leg temperature was closely coupled to the steam generator temperature during the transient, as shown in Figure 29. The reactor cooldown following the LOSP was primarily caused by the flow of EFW into the steam generator. The sensitivity of the response of the reactor coolant system to EFW flow is illustrated by Figures 23, 24, and 33.

5. Natural circulation was fully established in the calculations when the coastdown of the reactor coolant pumps was completed.

   Natural circulation was indicated when the loop flows stabilized after the reactor coolant pumps stopped spinning. The transition from forced convection to natural circulation was smooth in all the calculations performed. Once established, natural circulation never stopped.

6. The magnitude of the natural circulation flow was sensitive to EFW.

   As illustrated by Figure 28, the natural circulation flow decreased nearly 50% when EFW was stopped and then increased nearly 40% when EFW was restarted. When EFW was on, most of the heat transfer occurred near the EFW injection location at the top of the steam generator. When EFW was off, most of the heat transfer occurred below the mixture level, which was located in the bottom half of the steam generator. The location of the heat transfer affected the temperature distribution of the reactor coolant in the steam generator tubes. The temperature distribution affected the gravitational head that caused natural circulation.

7. Natural circulation flow was modestly sensitive to HPI.

   The natural circulation flow was about 6% higher in a calculation without HPI compared to a calculation with HPI, as shown in

Figure 32. However, loop temperature difference, an indicator of natural circulation, was significantly affected by HPI as shown in Figure 31.

8. Natural circulation flow was modestly sensitive to opening the steam generator ADVs.

   Figure 36 shows that the natural circulation flow was about 13% lower in a calculation with the ADVs closed compared to a calculation with the ADVs open.

9. Opening the ERV did not significantly affect natural circulation.

   The ERV was only open for about 10 s, not long enough to affect loop temperature distribution and natural circulation.

10. The presence of natural circulation could be inferred from temperature measurements.

    The steam generator and cold leg temperatures were closely coupled during natural circulation. The hot leg temperature also responded to changes in steam generator temperature, although the response was delayed for a few minutes because of transit time effects. The difference between hot and cold leg temperatures stabilized shortly after natural circulation was established.

5. REFERENCES

1. Arkansas Power and Light Company, Arkansas Nuclear One-Unit 1 Final Safety Analysis Report, Docket No. 50-313.

2. W. D. Lanning, Report on Loss of Offsite Power Event at Arkansas Nuclear One, Units 1 and 2 on April 7, 1980, Office for Analysis and Evaluation of Operational Data, Nuclear Regulatory Commission, October 15, 1980.

3. V. H. Ransom et al., RELAP5/MOD1.5: Models, Develomental Assessment, and User Information, EGG-NSMD-6-35, October 1982.

4. P. D. Bayless, Analysis of the June 24, 1980 Loss of Off-site Power Transient at Arkansas Nuclear One Unit 2, EGG-NTAP-6309, June 1983.

5. C. D. Fletcher et al., RELAP5 Thermal-Hydraulic Analysis of Pressurized Thermal Shock Sequences for the Oconee-1 Pressurized Water Reactor, EGG-NSMD-6343, July 1983.

6. "Decay Heat Power in Light Water Reactors," American Nuclear Society, ANSI/ANS-5.1-1979, Lagrange Park, Illinois, August 1979.

7. Evaluation of SBLOCA Operating Procedures and Effectiveness of Emergency Feedwater Spray for B&W-Designed Operating NSSS, B&W Doc. ID. 77-1141270-00, February 1983.

NRC FORM 335 (11-81)

U.S. NUCLEAR REGULATORY COMMISSION

BIBLIOGRAPHIC DATA SHEET

1. REPORT NUMBER *(Assigned by DDC)*: EGG-SAAM-6381

4. TITLE AND SUBTITLE: Analysis of the April 7, 1980 Loss of Off-Site Power Transient at Arkansas Nuclear One Unit 1

2. *(Leave blank)*

3. RECIPIENT'S ACCESSION NO.

7. AUTHOR(S): C. B. Davis

5. DATE REPORT COMPLETED: MONTH August YEAR 1983

9. PERFORMING ORGANIZATION NAME AND MAILING ADDRESS *(Include Zip Code)*

EG&G Idaho, Inc.
Idaho Falls, ID 83415

DATE REPORT ISSUED: MONTH August YEAR 1983

6. *(Leave blank)*

8. *(Leave blank)*

12. SPONSORING ORGANIZATION NAME AND MAILING ADDRESS *(Include Zip Code)*

Office for Analysis and Evaluation of Operational Data
U.S. Nuclear Regulatory Commission
Washington, DC 20555

10. PROJECT/TASK/WORK UNIT NO.

11. FIN NO.: A6270

13. TYPE OF REPORT: Technical

PERIOD COVERED *(Inclusive dates)*

15. SUPPLEMENTARY NOTES

14. *(Leave blank)*

16. ABSTRACT *(200 words or less)*

The loss of off-site power transient that occurred at Arkansas Nuclear One Unit 1 on April 7, 1980 was analyzed using the RELAP5 computer code. The transient was analyzed to understand the plant response, particularly in relation to natural circulation. Calculations were performed to determine the sensitivity of the plant response to high pressure injection, emergency feedwater, and the operation of the steam generator atmospheric dump valves. Methods of identifying the presence of natural circulation were investigated.

17. KEY WORDS AND DOCUMENT ANALYSIS

17a. DESCRIPTORS

17b. IDENTIFIERS/OPEN-ENDED TERMS

18. AVAILABILITY STATEMENT: Unlimited

19. SECURITY CLASS *(This report)*: Unclassified

21. NO. OF PAGES

20. SECURITY CLASS *(This page)*: Unclassified

22. PRICE: $